Aus dem Institut für Immunologie
Institut der Ludwig-Maximilians-Universität München

The Origin of Memory B Cells

Dissertation
zum Erwerb des Doktorgrades der Medizin
an der Medizinischen Fakultät der
Ludwig-Maximilians-Universität München

vorgelegt von
Tobias Wirthmiller

aus
Hallein

Jahr
2025

Mit Genehmigung der Medizinischen Fakultät der
Ludwig-Maximilians-Universität zu München

Erster Gutachter:	*Prof. Dr. rer. nat. Ludger Klein*
Zweiter Gutachter:	Prof. Dr. Michael Meyer
Dritter Gutachter:	Prof. Dr. Tobias Herold
ggf. weitere Gutachter:	Priv. Doz. Dr. Franziska Thaler

Dekan:	Prof. Dr. med. Thomas Gudermann

Tag der mündlichen Prüfung:	24.03.2025

Table of Contents

Zusammenfassung:

Plasmazellen und B-Gedächtniszellen stellen die Bausteine eines langlebigen Immunsystems dar. Ihre Erforschung ist zentral für ein besseres Verständnis grundlegender Infektionsgeschehen im menschlichen Körper. Plasmazellen und B-Gedächtniszellen galten lange als Produkt eines Keimzentrums im lymphatischen Gewebe. In den letzten Jahrzehnten konnten verschiedene Arbeitsgruppen in Mäusen, denen ein Keimzentrum fehlt, die Produktion von B-Gedächtniszellen nachweisen.

Diese Beobachtungen warfen die Frage auf, ob B-Gedächtniszellen in Mäusen ohne Keimzentrum eine unphysiologische Reaktion auf das Fehlen eines Keimzentrums darstellen oder ob in Mäusen mit einem Keimzentrum B-Gedächtniszellen unabhängig vom Keimzentrum produziert werden. Manche Arbeitsgruppen beobachteten B-Gedächtniszellen in Mäusen, die ein Keimzentrum bilden können, bevor dieses entstanden ist (das Keimzentrum bildet sich zirka drei bis vier Tage nach Immunisierung). Diese Forschungsergebnisse legen die Existenz einer zweiten Subgruppe von B-Gedächtniszellen, die unabhängig eines Keimzentrums gebildet werden, nahe.

Es bleibt jedoch die Frage bestehen, ob diese keimzentrumsunabhängigen B-Gedächtniszellen auch nach der Bildung eines Keimzentrums weiterhin produziert werden. Eine Herausforderung liegt in der Schwierigkeit, die Population der keimzentrumsunabhängigen von den keimzentrumsabhängigen B-Gedächtniszellen zu unterscheiden. Letzteres ist vor allem auf das Fehlen geeigneter Zelloberflächenmarker zur Differenzierung zurückzuführen.

Um dieses Hindernis zu umgehen, verwendeten wir ein Mausmodell, das eine Rückverfolgung von B-Zellen anhand ihrer Abstammung erlaubt. Das von uns genutzte Mausmodell kann Auskunft über die Anzahl der Teilungen einer B-Zelle geben. Da B-Zellen sich im Keimzentrum deutlich häufiger teilen als außerhalb des Keimzentrums, schließen wir in dieser Studie vom Teilungsverhalten (gemeinsam mit anderen Faktoren wie der Mutationsrate der B-Zellen) auf einen stattgefundenen Aufenthalt im Keimzentrum. Hiermit können keimzentrumsunabhängige von keimzentrumsabhängigen B-Gedächtniszellen unterschieden werden. Eine Limitation dieses Modells besteht darin, dass aufgrund des Teilungsverhaltens und Faktoren wie der Mutationsrate auf einen Aufenthalt im Keimzentrum zwar mit einiger Gewissheit geschlossen, dieser aber nicht definitiv nachgewiesen werden kann.

Unsere Resultate weisen darauf hin, dass während der gesamten Immunreaktion (genauer gesagt mindestens der ersten 30 Tage) B-Gedächtniszellen des keimzentrumsunabhängigen und keimzentrumsabhängigen Typs in Mäusen mit einem funktionierenden Keimzentrum produziert werden. Die Daten zeigen eine geringere Anzahl an Mutationen in den Antikörpergenen bei keimzentrumsunabhängigen B-Gedächtniszellen im Vergleich zu keimzentrumsabhängigen B-Gedächtniszellen. Da sich B-Zellen im Keimzentrum häufiger teilen und Mutationen erwerben, wirkt dieses Resultat übereinstimmend mit bisherigen Forschungsergebnissen. Beinahe alle (über 98 %) der keimzentrumsunabhängigen B-Gedächtniszellen wiesen einen B-Zell-Rezeptor vom Typ Immunglobulin M auf, während keimzentrumsabhängige B-Gedächtniszellen etwa zur einen Hälfte ein Immunglobulin vom Typ M aufzeigten und zur anderen Hälfte bereits einen Klassenwechsel vollzogen hatten. In vielen Studien werden Funktionsweisen von B-Gedächtniszellen an den Klassentyp der Zelle gebunden.

Es wäre daher eine mögliche Interpretation, dass keimzentrumsunabhängige B-Gedächtniszellen aufgrund ihres fast durchgehend vorhandenen Immunglobulin-M-Typs bei Re-Exposition durch einen Erreger vorwiegend an der Gründung neuer Keimzentren beteiligt sind.

Darüber hinaus zeigten Experimente mit Einzelzellanalysen, dass keimzentrumsabhängige B-Gedächtniszellen von Einzelzellen und nicht von dominanten Klonen im Keimzentrum abstammen.

Zusammenfassend konnten wir in dieser Studie sowohl die kontinuierliche Produktion von keimzentrumsabhängigen und keimzentrumsunabhängigen B-Gedächtniszellen in Mäusen mit einem intakten Immunsystem zeigen als auch Unterschiede der zwei Populationen in Mutationszahl und Klassentyp darstellen.

Abstract

Plasma cells and memory B cells are the building blocks of a long-lived immune system. Their research is central to a better understanding of basic infectious processes in the human body. Plasma cells and memory B cells were long thought to be the product of germinal centers in lymphoid tissue. In recent decades, several research groups have demonstrated the production of memory B cells in mice lacking a germinal center.

These observations raised the question of whether memory B cells in mice without a germinal center represent a non-physiological response to the absence of a germinal center or whether memory B cells are produced independently of the germinal center in mice with a germinal center. Some research groups have observed memory B cells in mice that are capable of forming a germinal center before its formation (the germinal center forms approximately 3-4 days after immunization). These research results suggest the existence of a second subset of memory B cells that are formed independently of a germinal center.

However, the question remains whether these germinal center-independent memory B cells continue to be produced even after the formation of a germinal center. One challenge lies in the difficulty of distinguishing the population of germinal center-independent memory B cells from germinal center-dependent memory B cells. This is mainly due to a lack of suitable cell surface markers for differentiation.

To overcome this obstacle, we used a mouse model that allows tracing B cells based on their lineage. The mouse model we use can provide information about the number of divisions of a B cell. Since B cells divide significantly more frequently in the germinal center than outside the germinal center, in this study we infer from the division behavior (together with other factors such as the mutation rate of the B cells) that a stay in the germinal center has taken place. This allows us to distinguish germinal center-independent from germinal center-dependent memory B cells. A limitation of this model is that, although it can be concluded with some certainty that a stay in the germinal center has taken place based on the division behavior and factors such as the mutation rate, this cannot be definitively proven.

Our results indicate that memory B cells of the germinal center-independent and germinal center-dependent type are produced in mice with a functional germinal center throughout the immune response (more precisely, at least the first 30 days). The data show a lower number of mutations in the antibody genes in germinal center-independent memory B

cells compared to germinal center-dependent memory B cells. Since B cells in the germinal center divide and acquire mutations more frequently, this result is consistent with previous research findings. Almost all (over 98 %) of the germinal center-independent B memory cells have an immunoglobulin M-type B cell receptor, while about half of the germinal center-dependent B memory cells had an M-type immunoglobulin and the other half had already undergone a class switch. In many studies, the functions of memory B cells are linked to the isotype class of the cell.

It would, therefore, be a possible interpretation that germinal center-independent memory B cells are predominantly involved in the establishment of new germinal centers upon re-exposure to a pathogen due to their predominant immunoglobulin M type.

Furthermore, single-cell analysis experiments showed that germinal center-dependent memory B cells are derived from single cells, not dominant clones in the germinal center.

In summary, this study showed the continuous production of germinal center-dependent and germinal center-independent memory B cells in mice with an intact immune system and demonstrated differences in mutation number and class type between the two populations.

List of Figures

List of Abbreviations

4-Hydroxy-3-nitrophenylacetyl hapten	NP
adaptive immune response	AIR
antigen	Ag
antigen-presenting cell	APC
B cell receptor	BCR
CellTrace™ Violet	CTV
chicken gamma globulin	CGG
cluster of differentiation	CD
collagen type 1, alpha 1	Col1a1
complementary deoxyribonucleic acid	cDNA
coronavirus disease 2019	COVID-19
dark zone	DZ
dendritic cell	DC
deoxyribonucleic acid	DNA
double negative	DN
double positive	DP
doxycycline	DOX
estrogen receptor T2	ERT2
fluorescence-activated cell sorting	FACS
follicular B cell	FBC
follicular dendritic cell	FDC
germinal center	GC
human immunodeficiency virus	HIV
immunoglobulin	Ig
immunoglobulin heavy chain	IgH
immunoglobulin kappa chain	IgK
immunoglobulin light chain	IgL
innate immune response	IIR
light zone	LZ
lymph node	LN

lymphotoxin alpha	LTα
major histocompatibility complex	MHC
marginal zone B cell	MZC
memory B cell	MBC
messenger ribonucleic acid	mRNA
peptide major histocompatibility complex	pMHC
phycoerythrin	PE
plasma cell	PC
polymerase chain reaction	PCR
Rosa 26	R26
ribonucleic acid	RNA
severe acute respiratory syndrome coronavirus type 2	SARS-CoV-2
single positive	SP
somatic hypermutations	SHM
sphingosine-1-phosphate receptor 2	S1pr2
tamoxifen	TAM
tetracycline operator	TetO
tetracycline transactivator element	tTA
Zoanthus sp. green fluorescent protein	ZsGreen

List of Tables

1. Introduction

1.1 Immune System

Through a communication network of cells, lymphoid organs, molecules and their mediated biological processes, the human immune system protects against more than 1400 species of human pathogens (Woolhouse and Gowtage-Sequeria, 2005). These include viruses, bacteria, fungi and parasites. In 2019, infectious syndromes caused around 13 million deaths worldwide (Gray and Sharara, 2022).

Using vaccinations to stimulate the immune system has enabled the eradication of infectious diseases such as smallpox in humans (Fenner et al., 1988) and rinderpest in ruminants (Roeder et al., 2013). As of December 2021, the severe acute respiratory syndrome coronavirus type 2 (SARS-CoV-2) has infected more than 280 million people and caused 5.4 million deaths (Msemburi et al., 2023). The virus's novelty to our immune system and its high transmission rate allowed it to spread with unprecedented speed, resulting in a global ‘lockdown’ as the only feasible countermeasure (Morens and Fauci, 2020). This led to a spike in research on coronavirus disease 2019 (COVID-19). Twelve vaccines have obtained an Emergency Use Listing by the World Health Organization as of December 2022 (Mathenge et al., 2023). Several novel vaccine technologies, including mRNA-based COVID-19 vaccines (Baden Lindsey R. et al., 2021; Polack et al., 2020), have been utilized in development and proven effective against COVID-19 (Dagan et al., 2021). However, a common problem with viruses is their ability to develop ‘escape’ mutations that may allow them to evade the immune response elicited by vaccination (Garcia-Beltran et al., 2021; Lucas et al., 2001). This development was seen with the emergence of SARS-CoV-2 variants (Chakraborty et al., 2022; Garcia-Beltran et al., 2021) and showed a reduction in vaccine efficacy for these variants *in vitro* (Chen et al., 2021; Wang et al., 2021). Vaccine protection strongly correlates with the induction of specific antibodies (Plotkin, 2010), which are produced by long-lasting plasma cells (PC) and memory B cells (MBC).

Furthering our understanding of immune responses and the mechanisms underlying long-lasting immunity may substantially aid the development of modern and effective vaccines (Akkaya et al., 2020).

Regardless of the site within the body, the mammalian immune system offers defense against pathogen invasion. The immune organs involved in the immune response can be

grouped into primary and secondary lymphoid organs. Immune organs and lymph vessels represent the infrastructure of the immune network. Within this infrastructure lie many layers of defense that can roughly be attributed to two distinct systems protecting us from pathogens: the innate and the adaptive immune system (see section 1.2).

Primary lymphoid organs include the bone marrow and thymus, where special immune cells called lymphocytes are produced. They can further be divided into B- and T lymphocytes. B lymphocytes (also called B cells) are named after the bursa fabricii in birds, not the bone marrow, as commonly thought (Cooper et al., 1965; Glick et al., 1956; Roitt et al., 1969). T lymphocytes are named after the thymus (Roitt et al., 1969). Secondary lymphoid organs include the spleen, tonsils, lymph nodes (LN) and mucosa-associated lymphatic tissue, such as tonsils, Peyer's patches and the appendix vermiformis (Figure 1). While primary lymphoid organs facilitate the production and maturation of lymphocytes in the absence of antigen (Ag), secondary lymphoid organs represent a collection site for pathogens. They are essential in triggering immune responses (Ruddle and Akirav, 2009).

Ags are any substance recognized by the adaptive immune system (see section 1.2.2). Typical Ags include proteins, glycoproteins and polysaccharides from pathogens (Murphy and Weaver, 2018).

Ags from pathogens can reach secondary lymphoid organs with the lymphatic fluid through the lymphatic system (Ruddle and Akirav, 2009). The lymphatic system entails a network of vessels of varying sizes connected to the LNs and other lymphoid organs (Figure 1; vessels in green). It is involved in the homeostasis of blood and tissue volume (Taylor et al., 1973) and immune cell trafficking (Angeli and Randolph, 2006; Johnson et al., 2006; Randolph et al., 2005). Every day, capillaries leak fluid into the extravascular compartments (Renkin, 1986) that contains nutrients for the cells but also Ags and immune cells that capture Ag from pathogens in the periphery of the body (Santambrogio, 2013). The lymph system collects fluid from extravascular compartments. It transports it back to the blood circulation while passing through LNs and lymphoid organs (Scallan et al., 2016), which serve as a filter station for Ag from pathogens (Bogoslowski and Kubes, 2018).

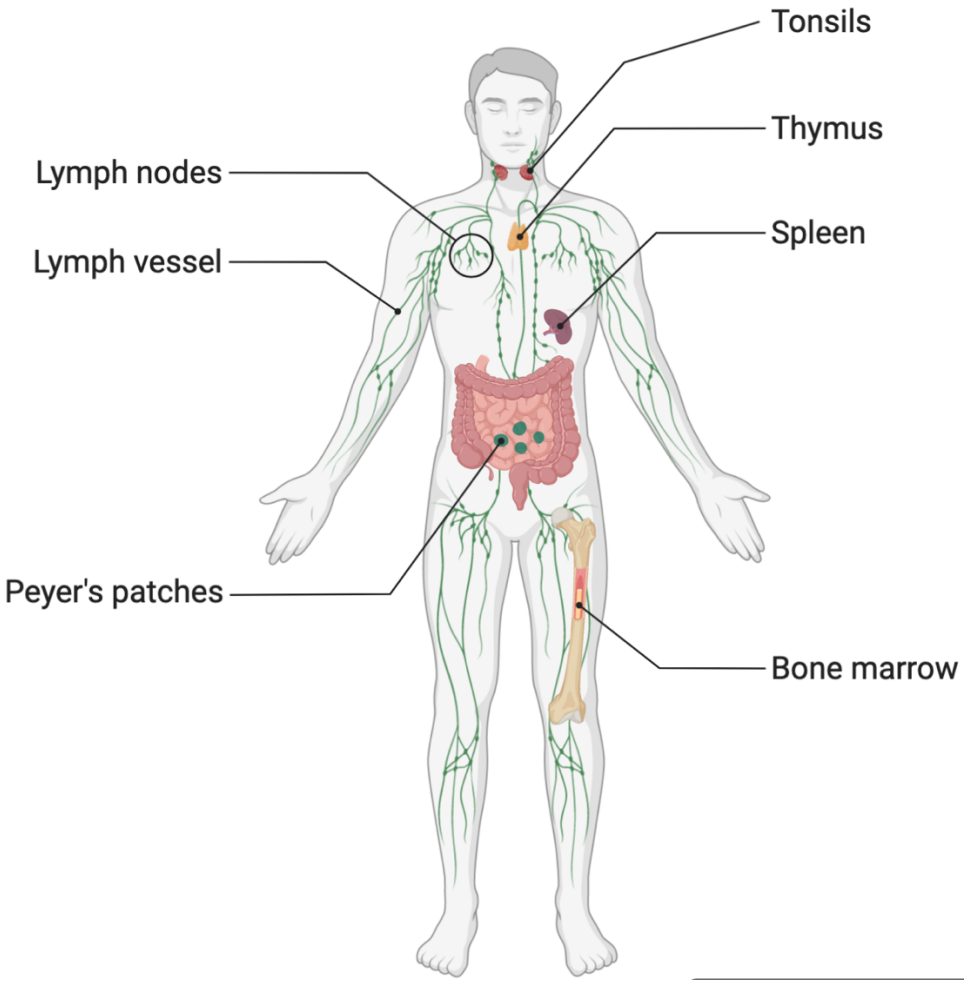

Figure 1 Schematic Distribution of Immune Organs in the Human Body: The figure shows lymph nodes, lymph vessels, Peyer's patches, tonsils, the thymus, the spleen and the bone marrow. Figure created with Biorender.com.

1.1.1 Difference Between Human and Murine Immune System

Using information from one species to understand the same processes of another species is the foundation for comparative medicine. Immunological functions are studied in various animal species as part of basic biomedical research. After understanding these same processes in animals, this knowledge is applied to understanding them in humans (Bryda, 2013). Mice constitute the most common research animal due to their small size, short reproductive cycle, short lifespan, an abundance of information concerning their anatomy, genetics, biology and physiology and the prospect of creating genetically modified mice (Hickman et al., 2017). Much of the human immune system knowledge is derived from *in vivo* research conducted in mice (Dunn, 1954). By injecting mice with an Ag, the formation of an immune response can be studied. One example is the injection with TM4-Core, a modified human immunodeficiency virus (HIV) envelope Ag (McGuire et al., 2016), used in this study to elicit an immune response in mice.

While sharing many similarities, mice and humans both possess a spleen, thymus, LNs and bone marrow (Dunn, 1954), they also exhibit distinct differences in areas like lymphocyte development, immune cell surface receptors and leukocyte transit time (Mestas and Hughes, 2004). Anatomically, mice have significant bronchus-associated lymphoid tissue. Mestas et al. argue this could result from a higher Ag intake through breathing as their head is closer to the ground (Mestas and Hughes, 2004).

There are also significant variations in LNs between mice and humans. The latter have around 1000 LNs (Qatarneh et al., 2006), while mice retain 22 LNs (Van den Broeck et al., 2006). Humans have more LNs that can drain proportionately smaller areas of tissue (Haley, 2003). Larger LNs in mice can typically be found as a single or double LN in the following locations: superficial and deep cervical, brachial, thoracic and mediastinal, axillary, pancreatic, renal, mesenteric, inguinal, lumbar and popliteal (Dunn, 1954).

1.1.2 Lymph Nodes

LNs are secondary lymphoid organs functioning as filter stations for the lymph fluids. Morphologically, human LNs have an oval shape and range in size up to 1,5 cm depending on their location in the body (Bontumasi et al., 2014).

The LN is surrounded by a capsule and can histologically be divided into a 1. cortex (Figure 2; light purple), 2. paracortex (Figure 2; dark purple) and 3. medulla. The cortex contains lymph follicles populated with B lymphocytes, whereas in the paracortical area, T lymphocytes reside. The capsule projects trabeculae into the LN, sectioning the LN into different lobules. Between the cortex and the capsule is the subcapsular sinus. The afferent lymph vessels bring lymph to the subcapsular sinus, which drains into the cortical sinus and eventually into the medulla, where the lymph will exit the LN at the hilum via efferent lymphatic vessels. Arteries and veins also enter and leave the LN via the hilum. The paracortical region contains postcapillary high endothelial venules. These vessels are the doorway for intravascular lymphocytes to enter the LN (for more details on LNs, see Willard-Mack, 2006)

The LN acts as a barrier to pathogens in the lymph and filters the incoming lymphatic fluid carrying Ags, antigen-presenting cells (APC), growth factors, cytokines and serum proteins. Resident immune cells in the LN can collect foreign Ag and present it to B cells. B cells can then initiate a robust immune response by founding germinal centers (GC),

an anatomical structure capable of generating antibody-producing PCs and MBCs (Bogoslowski and Kubes, 2018).

GCs were first described in 1884 by Walter Flemming (Nieuwenhuis and Opstelten, 1984). He discovered small zones within the LN that contain extremely high numbers of dividing lymphoid cells. Here, B lymphocytes multiply after Ag contact through clonal expansion and enhance their affinity through somatic hypermutations (SHM) (Jacob et al., 1991), which will be explained in section 1.3.

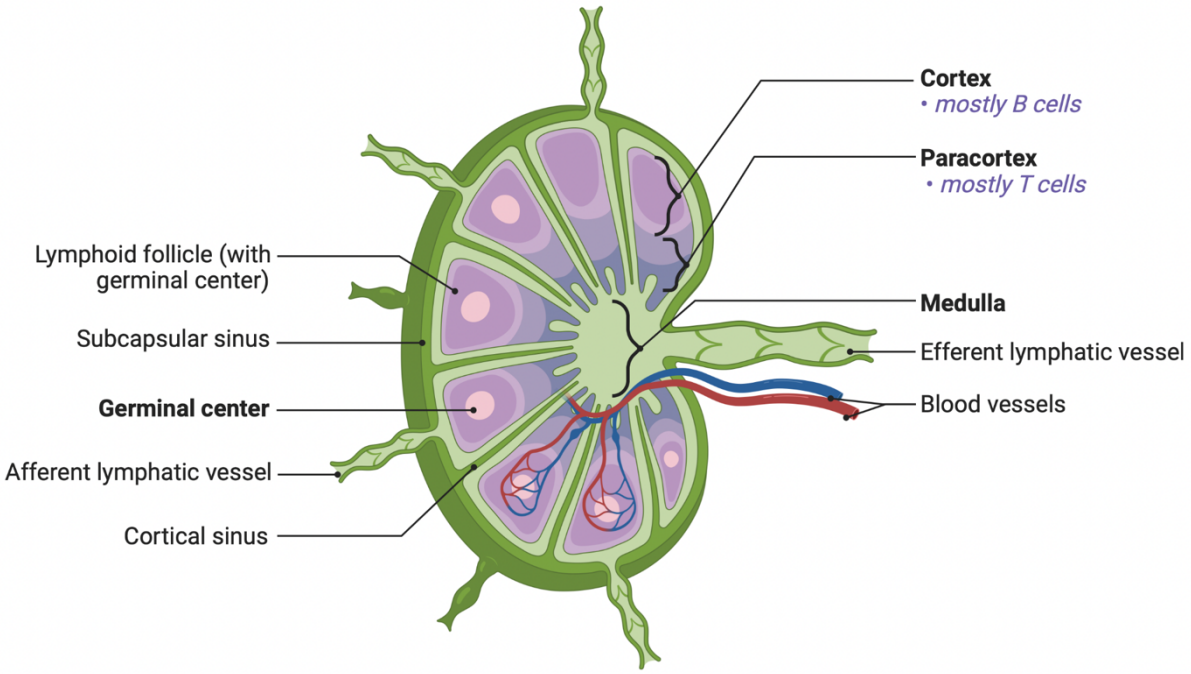

Figure 2 Structure of a Human Lymph Node: The figure shows the germinal center, cortex, paracortex and other structures in the lymph node. The capsule is marked in green. Figure created with Biorender.com

1.2 Immune Responses to Pathogens

The innate immune response (IIR) is the first layer of immune defense to respond to the pathogen's presence, as it can engage with the foreign Ag within minutes. The fast response of the IIR is possible due to its large pool of conserved microbial components known to humans. It acts as a first line of defense until the adaptive immune response (AIR) is set in motion. The AIR, while specific, is slow and takes between 3-5 days to engage following Ag exposure. It can develop a tailored immune response by producing cells that have a high affinity to the Ag of the invader (see Kaur and Secord, 2019 for more information).

1.2.1 Innate Immune Response

While the AIR requires time to develop a response, agents of the innate immune system engage the threat. These can be divided into cells (natural killer cells, macrophages, dendritic cells (DC) and granulocytes) and humoral agents (naturally occurring antibodies, complement cascades and pentraxins such as the C-reactive protein; Kaur and Secord, 2019).

The skin constitutes the first stage of defense. While not only imposing as a physical barrier to dirt and foreign organisms, it can actively fight off invaders with its surface covered in antimicrobial peptides and immune cells located in the epidermis (Chambers and Vukmanovic-Stejic, 2020). Due to the IIR's ability to recognize conserved microbial components, it can efficiently carry out its role as a first line of defense. The immune cells of the epidermis can: 1. Present Ags from invaders to resident T cells and initiate a local immune response; and 2. migrate to the LN and trigger a systematic adaptive immune response (Collin and Bigley, 2018). If the IIR can clear the pathogen before reaching secondary lymphoid organs, the AIR will not be activated (Kaur and Secord, 2019). Immune cells capable of presenting Ags are known as APCs and include DCs, macrophages, B cells and Langerhans cells. Except for B cells, these APCs can be found in the skin (Kashem et al., 2017).

1.2.2 Adaptive Immune Response

If the IIR cannot clear the threat, the AIR is engaged in germ neutralization. The key agents of the AIR are B and T lymphocytes, as well as antibodies. The AIR can roughly be classified into 1. T cell-mediated immunity and 2. humoral immunity. Humoral immunity is achieved by B cells, their derivates (plasmablast, PC and MBC) and antibodies.

Recently, with the description of innate B cells and innate lymphoid cells that show properties initially associated with the innate system (e.g., Ag internalization, regulatory B cell functions and capacity to activate classical complement pathway), authors like Hillion et al. have suggested reevaluating the dichotomy of innate and adaptive systems (Hillion et al., 2020). For simplicity, the two systems will, however, be introduced separately in this work.

1.2.2.1 T Cell-Mediated Immunity

Lymphocytes are leukocytes (= white blood cells). Other leukocytes include basophils, eosinophils and monocytes. Lymphocytes are the second largest population of leukocytes

in humans, with 20-40%, after neutrophils, constituting between 50-70% (Pal, 2006). In mice, the distribution is somewhat different, with 75-90% of leukocytes being lymphocytes and only 10-25% neutrophils (for more details, see Mestas and Hughes, 2004). T and B lymphocytes are morphologically indistinguishable but show distinct receptor makeup and functionality varieties.

T lymphocytes originate from bone-marrow-derived progenitor cells that undergo a series of maturation and selection steps within the thymus. After these maturation processes, they are released into the blood and lymph circulation as mature yet still naïve T lymphocytes. Mature T lymphocytes remain naïve until an APC presents an Ag to them in a process called 'priming,' which triggers their differentiation into T effector lymphocytes. These include several subtypes, such as $CD4^+$ T helper cells or $CD8^+$ cytotoxic T cells. CD is an abbreviation for Cluster of Differentiation, a family of molecules present at the surface of immune cells. The Ag receptor of T cells can recognize foreign Ags on other cells if bound to a particular cell surface protein/molecule called major-histocompatibility-complex (MHC). The MHC gene family can be divided into three subclasses. MHC I class genes encode for molecules on all nucleated cells and platelets, e.g., all cells except red blood cells. MHC II class genes encode for molecules mostly found on APCs. MHC III class molecules are involved in the complement system's response. The multimer that results after an Ag peptide is bound to the MHC is called peptide major histocompatibility complex (pMHC).

$CD8^+$ cytotoxic T cells recognize foreign Ags from cells carrying the MHC-I molecule and can neutralize infected cells. CD4 helper cells can build a wide range of subtypes, such as T helper cells 1, 2 and 17, T follicular helper cells and T regulatory cells (Murphy and Weaver, 2018). They are essential in establishing and maintaining an immune response (Kumar et al., 2018).

1.2.2.2 B Cells and Antibody-Driven Humoral Immunity

B lymphocyte production in humans occurs mainly in the liver until the mid-second trimester (Popescu et al., 2019) before the bone marrow becomes the dominant production site (Holt and Jones, 2000). Once maturation of B lymphocytes in the bone marrow has been completed, B cells exit the bone marrow. B cells at this stage are developmentally mature but are considered naïve cells as they have not made Ag contact yet. These B cells can be grouped into three subtypes depending on the location they will populate. The most common of these cells are called follicular B cells (FBC), as they inhabit the lymph

follicles of LNs and the spleen. The second type, B1 B cells, populate peritoneal and pleural cavities and mucosa tissue. Marginal zone B cells (MZC) constitute the third subtype and can be found in the marginal zone of the spleen (Allman and Pillai, 2008). B1 and MZC's contribution to the PC's fate is poorly characterized (Nutt et al., 2015). Thus, the following section will focus on describing the progression of FBCs towards the PC fate.

To activate a B cell, contact with an Ag and $CD4^+$ T cell help is required (Parker, 1993). FBCs can interact with Ags in several ways. One option is the acquisition of soluble Ag passing through the LN (Pape et al., 2007). This is the case for smaller Ags that can exit the subcapsular sinus of the LN (see Figure 2) through small gaps without additional help from APCs (Gretz et al., 2000). Capturing cell-bound Ag from follicular DCs (Suzuki et al., 2009), lymphoid DCs (Gonzalez et al., 2010) or subcapsular macrophages (Carrasco and Batista, 2007) constitutes another possibility for Ag interaction. The latter is likely to occur for Ags too large to pass through the gaps of the subcapsular sinus, thus relying on APC-help (Carrasco and Batista, 2007).

Once the B cell receptor (BCR) recognizes an Ag, the B cell will internalize, process and present the Ag on its MHC-II molecule at the cell surface. It then migrates from the B cell follicle in the LN or spleen to the T cell border (between cortex and paracortical area in the LN) to receive signals from a T helper cell (Okada et al., 2005). T helper cells that have been exposed to the same Ag by an APC can now recognize the Ag presented on the MHC-II molecule of the B cell and initiate the B cell's activation (Vitetta et al., 1989).

T cell help is required for most B cells to become activated, but a few exceptions exist. Contact with multivalent Ags such as lipids (T cell-independent Type 1 Ag) or polysaccharides (T cell-independent Type 2 Ag) does not require T cell help. They can exhibit repetitive epitope sequences leading to cluttering of BCRs, which in turn triggers a T cell-independent B cell activation (Vos et al., 2000). Following this activation, B cells migrate to the area next to the marginal zone of the spleen or the outer follicle of the LN for a short period of proliferation (Coffey et al., 2009; Schwickert et al., 2011) before they: 1. differentiate into a plasmablast or 2. create a GC (see section 1.3).

Plasmablasts are antibody-secreting cells that constitute an early antibody response in the AIR (MacLennan et al., 2003). While the contribution of B1 B cells and marginal zone B cells to the PC pool is poorly characterized, they can develop into plasmablasts (Nutt et al., 2015). Several hypotheses about the determination of an activated B cell from the FB

cell lineage to found a GC or become a plasmablast exist. Porto et al. suggest that the fate of activated B cells to become GC cells or plasmablasts is determined stochastically (Porto et al., 1998). Another theorizes that activated B cells harboring high affinity to Ags are positively selected into the plasmablast compartment (Paus et al., 2006). Paus et al. have demonstrated that decreasing Ag affinity or Ag density leads to a diminished plasmablast response with minimal impact on the GC-reaction (Paus et al., 2006). Further knowledge on steering an immune response towards a GC-pathway or an extrafollicular plasmablast fate and its effects on the progress of infection would be beneficial to understand this process better.

Both plasmablasts and PCs are capable of producing immunoglobulins (Ig). Igs were first described by von Behring and Kitasato in 1890 while conducting experiments examining the rabbit's immunity against diphtheria and tetanus (von Behring and Kitasato, 1890; republished in 1991). They can be found in blood, spleen, interstitial fluids, bone marrow and mucosa-associated lymphoid tissue through exocrine secretion (Ma and O'Kennedy, 2015). Igs can recognize and bind to Ags, initiating several immunological pathways that lead to neutralization, opsonization, or complement activation (Murphy and Weaver, 2018). Igs have two heavy and light chains forming a 'Y'-like shape. Light chains have one constant and one variable region, whereas heavy chains have three constant and one variable region. The variable regions of heavy and light chains are responsible for the antibody's specificity and constitute the Ag binding site. In humans and mice, there are five Ig isotypes (IgM, IgD, IgG, IgA, or IgE), which are determined by their heavy chain. Table 1 provides an overview of Ig's role in the AIR.

Antibodies	Function	Reference
IgM	first antibody secreted after exposure to pathogens	Keyt et al., 2020
IgD	influences mucosal homeostasis by activating mast cells, basophils and monocytes	Gutzeit et al., 2018
IgG	complement activation; Fc-receptor mediated effector functions	Valenzuela and Schaub, 2018
IgA	first line of defense against mucosal pathogens	Kumar et al., 2020
IgE	involved in allergic reactions	Galli and Tsai, 2012

Table 1 Antibody Classes and Role in Adaptive Immune Response

The ability of the AIR to modify its components in a way that achieves specific and efficient immune responses is a hallmark of human immunology and its understanding builds

the foundation for developing novel therapeutics, such as monoclonal antibodies in the fight against cancer.

1.3 Germinal Center Formation

Upon activation, a B cell can either differentiate into a plasmablast or create a GC. Studies using adaptive cell transfer experiments in mice have shown that a T cell limited checkpoint regulates entry into the GC (Schwickert et al., 2011). B cells that will proceed to become GC cells (Pre-GC B cells) compete for Ags to present to T cells, which appear to preferentially give help to B cells with a higher density pMHC on their cell surface. The density of pMHC is usually a result of BCR affinity; thus, highly affinitive B cells can capture more Ag. They are positively selected by T cells and dominate the GC reaction (Schwickert et al., 2011).

While these results demonstrate that pre-GC B cell selection occurs based on B cell affinity, it has been shown that the absolute affinity threshold for entrance to the GC is generally very low (Schwickert et al., 2011; Akkaya et al., 2020). Therefore, even cells with lower affinity to an Ag, while not preferentially receiving T cell help, can enter the GC.

Before joining a GC, B cells can perform a switch of their BCR antibody class. While this can occur within the GC too, it was demonstrated that the majority of cells undergo this process after T cell priming before joining a GC (Roco et al., 2019). Once a B cell has entered a GC, it can obtain mutations (SHMs) that can enhance its affinity (Rajewsky, 1996). This process will lead to a high proliferation of the GC B cell (clonal expansion) (Rajewsky, 1996). GC cells express the Bcl6 gene that was demonstrated to be essential for GC formation as Bcl6-deficient mice were found to be unable to form a GC (Fukuda et al., 1997).

The GC can be divided into a dark zone (DZ) and a light zone (LZ). SHM, the principle underlying affinity maturation, and clonal expansion are both localized in the DZ (Figure 3) within the GC (Victora and Nussenzweig, 2012). The DZ harbors B cells expressing the activation-induced enzyme (Muramatsu et al., 2000), which causes random mutations in GC B cell genes encoding for the variable region of the antibody. Mutations in this region lead to affinity changes in the GC B cell. B cells that have obtained mutations will undergo clonal expansion and migrate to the LZ using a chemokine gradient. If a GC B cell acquires a damaged Ig during affinity maturation, it will undergo apoptosis (Mayer

et al., 2017) and be phagocytosed by resident macrophages (Swartzendruber and Congdon, 1963).

The LZ is populated with follicular dendritic cells (FDC) and follicular T helper cells. FDCs present Ags to the GC B cells coming from the DZ. GC B cells can capture Ags from FDCs and present them to follicular T helper cells for T cell help. This is part of the selection process determining the fate of a GC B cell. Multiphoton microscopy experiments in mice demonstrated that T cell help rather than competition for Ag from FDCs is likely to be the limiting factor for positive GC cell selection (Victora et al., 2010). Upon reception of T cell help, GC cells have three potential fates. Firstly, they can exit the GC as a PC. This fate is most common for cells, which develop a high affinity. Secondly, they can leave as MBCs. MBCs are predominantly generated from cells with lower affinity than PC precursor cells (Shinnakasu et al., 2016; Suan et al., 2017). Thirdly, they can re-enter the DZ to obtain further SHM and undergo more clonal expansion. A GC B cell can undergo many cycles between DZ and LZ before finally exiting the GC as a PC or MBC.

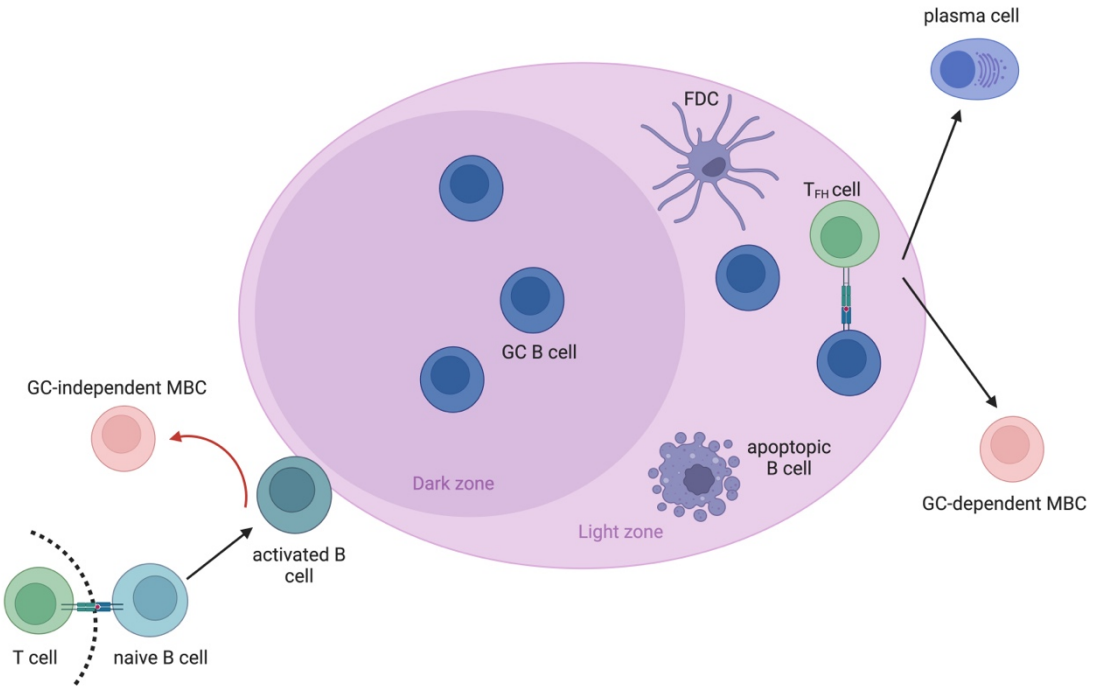

Figure 3 Mechanism of Germinal Center Formation: SHM and clonal expansion take place in the dark zone. The selection of GC cells takes place in the light zone. The figure shows two pathways for memory B cells: 1. The GC-independent memory B cell originating from activated B cells (see red arrow in the figure) and 2. the GC-dependent memory B cell originating from the GC. T_{FH} = T follicular helper cell. FDC = Follicular dendritic cell. GC = germinal center. The figure was created with Biorender.com.

1.4 Memory B Cells

Both long-lived PCs and MBCs are hallmarks of long-lasting immunity. A review by Akkaya et al. has described them as ‘two walls of protection against pathogens‘ (Akkaya et al., 2020). Upon Ag confrontation, long-lasting PCs produce antibodies against the pathogen. These long-lasting PCs are kept in the bone marrow once the infection has been fought off and the antibodies produced can be maintained for years, possibly even for a lifetime. If the body is exposed twice to the same pathogen, these antibodies react immediately, serving as a ‘first line of defense’. There are, however, situations when long-lived PCs deplete their antibody reservoirs or cannot recognize the pathogen anymore. In such cases, the ‘second wall of protection,’ namely MBCs, will take over (Akkaya et al., 2020).

GC cells may take on an MBC or PC fate under certain circumstances. Several markers are associated with MBC development: Bach2 (Shinnakasu et al., 2016), Ephrin-B1 (Laidlaw et al., 2017) and CCR6 (Suan et al., 2017). Common cell surface markers used for MBC identification include PDL-1, PDL-2, CD80, CD38, CD73, CD138, CD27 in humans and CD35 (Anderson et al., 2007; Good-Jacobson et al., 2010; Kaji et al., 2012; Klein et al., 1998; McHeyzer-Williams et al., 2000; Pape et al., 2011; Taylor et al., 2012). CD38 can distinguish MBCs, $CD38^+$, from GC cells, $CD38^-$ (Ridderstad and Tarlinton, 1998), but not MBCs from naïve B cells, as both are $CD38^+$ $GL7^-$ (Taylor et al., 2012). This creates a challenge for the detection of early IgM^+ MBCs.

It has also been shown that MBCs originate from cell groups localized close to the edge of the GC in the LZ (Laidlaw et al., 2017). Studies with precursor MBCs and precursor PCs further suggest that MBCs primarily arise from GC cells with a low affinity (Suan et al., 2017).

Upon leaving the GC, MBCs migrate through lymphoid organs like naive B cells. They remain quiescent until re-exposure to the pathogen, possibly even for life. When MBCs are exposed to a known Ag again, a secondary immune response is triggered and they can differentiate into PCs that produce Igs or rejoin a GC for further SHM and clonal expansion. As a result of MBCs, secondary immune responses can produce up to 100 times more B cells than primary responses (Murphy and Weaver, 2018).

It has long been assumed that MBCs can only be generated from GC cells within the GC. Previous studies have, however, demonstrated that MBCs can originate from a GC-independent pathway (see section 1.4.1).

1.4.1 Germinal Center-Independent Memory B Cells

As opposed to being the product of a linear development process, the early concepts of GC-independent MBCs resulted from studies pursuing various research questions. One of the first indications of this cell group was found in the work of Matsumoto et al., who studied mice lacking lymphotoxin alpha (LTα). LTα -/- mice cannot form a GC; nevertheless, Matsumoto et al. observed affinity maturation in antibody responses and somatic mutations in the nucleotides of antibody genes in LTα -/- mice. The findings suggest that affinity maturation may occur outside the GC, hinting at the possibility of MBCs independent of the GC (Matsumoto et al., 1996).

Several other researchers have observed secondary antibody responses in mice that cannot form a GC, including Blr1 (Förster et al., 1996) and Bcl6 (Toyama et al., 2002) deficient mice. Kaji et al. and Weisel et al. discovered cells with characteristics of MBCs before the formation of a GC in mice that can develop a GC (Kaji et al., 2012; Weisel et al., 2016). Taylor et al. have also reported GC-independent production of MBCs (Taylor et al., 2012). There is evidence for the production of GC-independent MBCs in humans as IgM^+ $CD27^+$ cells could arguably represent a human GC-independent MBC subset (Tangye and Good, 2007), but further studies are required for clarification. The above cited studies confirm the existence of GC-independent MBCs in mice; however, they have only been observed in mice without GCs or briefly in mice with GCs before GC formation.

Mice that cannot form a GC lack an intact immune system. It would be of critical interest to understand MBC formation in mice that can develop a GC, exhibit an intact immune system and allow the study of MBCs (GC-dependent and -independent) to be conducted in greater detail throughout the immune response. This work aimed to use an unbiased lineage-tracking system to follow the formation of MBCs within an intact murine immune system. We aspired to investigate the existence of GC-independent MBCs during a physiological immune response and assess the cell group's properties and characteristics using flow cytometry and single-cell RNA sequencing.

2. Material and Methods

2.1 Materials

Reagent/Resource	Source	Identifier
Mice		
Slpr2-ERT2cre	T. Kurosaki	Shinnakasu et al., 2016
Rosa-ZsGreen	Jackson Laboratory	Stock No 007906
VavTg-Col1a-mCherry	Nussenzweig Laboratory	Gitlin et al., 2014
Chemicals and recombinant proteins		
HIV-I TM4-Core	A. T. McGuire and L. Stamatatos; Fred Hutchinson Cancer Research Center, Seattle;	Dosenovic et al., 2015
Imject alum	Thermo Fisher Scientific	Cat#77161
Tamoxifen	Sigma	Cat#T5648
Corn oil	Sigma	Cat#C8267
Doxycyline	Sigma	Cat#D9891
Sucrose	Sigma	Cat#S0389-5KG
ACK lysing buffer	Gibco	Cat#A1049201
CD43 (Ly-48) MicroBeads	Miltenyi Biotec	Cat#130-049-801
TCL buffer	QIAGEN	Cat#1031576
2-Mercaptoethanol, BioUltra, for molecular biology, ≥99.0% (GC)	Sigma-Aldrich	Cat#M3148
RNAClean XP beads (RNA-SPRI beads)	Beckman Coulter	Cat#A63987
Random primers (14.5 ng/µl)	Invitrogen	Cat#48190-011
Tergitol type NP40	Sigma	Cat#NP40S
RNase inhibitor	Promega	Cat#N2615
Nuclease-free water	QIAGEN	Cat#1039498
Dithiothreitol (DTT)	Invitrogen	Cat#18080-044
SuperScript 111 First-Strand Synthesis Kit	Invitrogen	Cat#18080400
l0X buffer	QIAGEN	Cat# 203209

HotStarTaq DNA polymerase (5 units/µl)	QIAGEN	Cat#203209
Cresol Red	Sigma	Cat#C-9877
Ethanol 100% (meets USP specifications)	Decon Labs	Cat#2716
GelRed Nucleic Acid 10,000X in water	Biotium	Cat#41003
Live/dead marker Zombie NIR	BioLegend	Cat#423106
Fetal bovine serum	GE Healthcare Life Sciences	Cat#SH30910.03
0.5 M EDTA	Invitrogen	Cat#15575020
SeaKem LE Agarose	Lonza	Cat#50004
Software		
Biorender	Science Suite Inc.	www.biorender.com
Grammarly	Grammarly Inc.	www.grammarly.com
ChatGPT 4.0	OpenAI Inc.	www.openai.com/gpt-4
GraphPad Prism version 9	GraphPad Software	RRID: SCR_002798
FlowJo v10.3.5	FlowJo	RRID: SCR_008520
Adobe Illustrator CC 2018	BD Biosciences	RRID: SCR_014198
IgBlast tool (NCBI)	NCBI	RRID: SCR_002873
Devices		
FACSAria II cell sorter	BD Biosciences	N/A
SimpliAmp thermal cycler	Thermo Fisher Scientific	Cat#A24811
Illumina NovaSeq 6000	Illumina	N/A
Nextera XT DNA library preparation kit	Illumina	Cat# FC-131-1096
Flat Deck Thermo-Fast 96 detection plate	Thermo Fisher Scientific	Cat#AB1400W
Adhesive PCR sealing foil sheets	Thermo Scientific	Cat#AB0626

50 ml polypropenylene conical tube	Falcon	Cat#352070
Mini skirt PCR plates	Denville Scientific Inc.	Cat#18080-10
5 ml disposable serological pipette	Corning Inc.	Cat#4487
10 ml disposable serological pipette	Corning Inc.	Cat#4488
25 ml disposable serological pipette	Corning Inc.	Cat#4489
Cell strainer 70 µm	Falcon	Cat#352350
Insulin syringes	BD Biosciences	Cat#329461
Feeding tubes	Instech Laboratories	Cat#15155024
1 mL syringes with BD Luer-Lok	BD Biosciences	Cat#309628
DynaMag-96 side magnet	Thermo Fisher Scientific	Cat#12331D
BD LSRFortessa	BD Biosciences	N/A
BD FACSymphony	BD Biosciences	N/A

Table 2 Reagents or Resource including Source and Identifier

2.2 Primers

Primers for Sequencing, PCR 1 and PCR 2

AGGAACTGCAGGTGTCC	1st PCR IgH Forward 1mFH_I
CAGCTACAGGTGTCCACTCC	1st PCR IgH Forward 1mFH_II
TGGCAGCARCAGCTACAGG	1st PCR IgH Forward 1mFH_III
CTGCCTGGTGACATTCCCA	1st PCR IgH Forward 1mFH_IV
CCAAGCTGTGTCCTGTC	1st PCR IgH Forward 1mFH_V
TTTTAAAAGGTGTCCAGKGT	1st PCR IgH Forward 1mFH_VI
CCTGTCAGTAACTRCAGGTGTCC	1st PCR IgH Forward 1mFH_VII
TTTTAAAAGGGGTCCAGTGT	1st PCR IgH Forward 1mFH_VIII
CGTTCCTGGTATCCTGTCT	1st PCR IgH Forward 1mFH_IX
ATGAAGTTGTGGYTRAACTGG	1st PCR IgH Forward 1mFH_X
TGTTGGGGCTKAAGTGGG	1st PCR IgH Forward 1mFH_XI
AGAAGGTGTGCACACCGCTGGAC	1st PCR IgH Reverse 1mRG
AGGGGGCTCTCGCAGGAGACGAGG	1st PCR IgH Reverse 1mRM
RGTGCAGATTTTCAGCTTCCTGCT	1st PCR IgK Forward 1mFK_I
TGGACATGAGGGCYCCTGCTCAGT	1st PCR IgK Forward 1mFK_II
CTSTGGTTGTCTGGTGTTGAYGGA	1st PCR IgK Forward 1mFK_III
GTTGCTGCTGCTGTGGCTTACA	1st PCR IgK Forward 1mFK_IV
GTATCTGGTACCTGTGG	1st PCR IgK Forward 1mFK_V
TGCCTGTTAGGCTGTTGGTGCT	1st PCR IgK Forward 1mFK_VI

GCTCAGTTCCTTGGTCTCCTGTTGC	1st PCR IgK Forward mFK_VII
TGGGTGCTGCTGCTCTGGGT	1st PCR IgK Forward 1mFK_VIII
CAGTTCCTGTTTCTGTTARTGCTCTGG	1st PCR IgK Forward 1mFK_IX
TGCTCTGGTTATATGGTGCTGATGGG	1st PCR IgK Forward 1mFK_X
ACTGAGGCACCTCCAGATGTT	1st PCR IgK Reverse 1mRK
GGGAATTCGAGGTGCAGCTGCAGGAGTCTGG	2nd PCR IgH Forward 2mFG
GCTCAGGGAARTAGCCCTTGAC	2nd PCR IgH Reverse 2mRG
AGGGGGAAGACATTTGGGAAGGAC	2nd PCR IgH Reverse 2mRM
GAYATTGTGMTSACMCARWCTMCA	2nd PCR IgK Forward 2mFK
TGGGAAGATGGATACAGTT	2nd PCR IgK Reverse 2mRK

Table 3 Primers for Sequencing, PCR 1 and PCR 2. Primers previously published by von Boehmer et al., 2016

2.3 Mice

This study used a C57BL/6J background for all mutations. Animal procedures were conducted according to guidelines approved by Rockefeller University's institutional animal care and use committee.

A previous description of the VavTg-Col1a-mCherry mice was provided by Gitlin et al. (Gitlin et al., 2014), while Shinnakasu et al. (Shinnakasu et al., 2016) have described the S1pr2-ERT2cre mice, which were given by T Kurosaki (Laboratory of Lymphocyte Differentiation, Osaka University, Japan). Mice of the Rosa-ZsGreen strain (Ai6; Rosa-CAG-LSL-ZsGreen1-WPRE) were acquired from The Jackson Laboratory.

2.4 Immunizations and Administration of Tamoxifen and Doxycycline

The mice were immunized as follows: 5 µg TM4-Core (a HIV envelope Ag) diluted within 25 µl of PBS and precipitated in alum at a 2:1 ratio was injected into the footpads of the animal.

TM4-Core was provided by L. Stamatatos and Andrew T. McGuire. For activation of Cre recombinase, one dose of 12 mg tamoxifen diluted in 200 µl of corn oil was administered orally to mice as shown in Figure 11.

Doxycycline at a dose of 2 mg in 1x PBS was injected intraperitoneally to stop mCherry expression and initiate its dilution, which is necessary to distinguish cells by their number of divisions; 1g/liter doxycycline and 5% sucrose were added to the drinking water for six days thereafter.

2.5 Dissection of Mice and Flow Cytometry

Mice were euthanized using CO_2 overdoses and dissected to remove axillary and popliteal LNs. LNs were transferred to a 70 µm cell strainer placed on a six-well plate containing 5 ml FACS buffer (1x PBS, 10% fetal bovine serum, 2 mM EDTA). The six-well plate was kept on ice during the entire experiment. LNs were ground through the filter of the cell strainer, creating a single-cell suspension. The endpiece of a syringe was used to facilitate the grinding process. The cell suspension was aspirated with a 10 ml pipette and transferred to a 15 ml centrifuge tube. The filter was washed once more with 5 ml of FACS buffer and the wash was moved to the same 15 ml centrifuge tube to prevent losing cells stuck to the filter.

The tube was centrifuged at 350 g and 7°C for 5 minutes. The supernatant was discarded. 1 ml ACK lysis buffer was added to each well to lyse the erythrocytes contained in the sample. The tube was inverted two times and incubated for 1 minute to facilitate the lysing process. 10 ml FACS buffer was added to the tube to stop the lysis reaction. The content of the tube was transferred to a new 15 ml tube by pipetting through the filter of a new cell strainer. The tube was centrifuged at 350 g and 7°C for 5 minutes. The supernatant was discarded. The pellet was resuspended with drops of remaining supernatant left on the wall of the tube and transferred to a 96-well plate. Plate was centrifuged at 350 g and 7°C for 5 minutes. Supernatant was discarded.

Cells were then incubated with 5 µg/ml anti-CD16/32 on ice for 15 minutes to block Fc receptors. The Fc-block prevents antibodies from binding to the Fc-receptors of cells and thus avoids high background staining. During the Fc block incubation, the antibody mix for staining was prepared. The dilution factor of each antibody to the total mix volume can be seen in Table 4. Antibodies used (depending on the experiment) are listed in Table 4. Once Fc block incubation had finished, the 96-well plate was centrifuged at 350 g and 7°C for 5 minutes and the supernatant was removed. 100 µl antibody mix was added to each well. The plate was incubated on ice for 30 minutes, followed by centrifuging at 350 g and 7°C for 5 minutes. The supernatant was discarded. To perform flow cytometric analysis, we used the BD LSRFortessa and Symphony. For further details, see Viant et al., 2021.

Antibody	Antibody provider	Clone	Cat. No.
anti-IgM-e710 1/200 (final 1µg/ml)	Biosciences	R6-60.2	550881
anti-IgD-BV786 1/200 (final 1µg/ml)		11-26c.2a	563618
anti-CD95-PE-Cy7 1/200 (final 1µg/ml)		Jo2	557653
anti-CD38-PB 1/100 (final 5µg/ml)	Biolegend	90	102719
anti-B220-BV605 1/200 (final 1µg/ml)		RA3-6B2	103244
anti-T and -B cell activation antigen-e660 1/100 (final 2µg/ml)	eBiosciences	GL7	50-5902-82
anti-CD4-eF780 1/200 (final 1µg/ml)		RM4-5	47-0042-82
anti-CD8-eF780 1/200 (final 1µg/ml)		53-6.7	47-0081-82
anti-NK1.1-eF780 1/200 (final 1µg/ml)		PK136	47-5941-82
anti-F4/80-eF780 1/200 (final 1µg/ml)		BM8	47-4801-82
anti-mouse CD16/32(ratmAB 2.4G2, mouse Fc block) 1/500 (final 1µg/ml)	BD Biosciences	2.4G2	553141

Table 4 Flow Panel

2.6 RNA Purification and cDNA Synthesis

B cells from draining LNs were negatively enriched with CD43 (Ly-48) MicroBeads, stained and single-cell sorted in 96-well plates by using a FACSAria II. Cells were put in 5 µl TCL lysis buffer that contained 1% 2-beta-mercaptoethanol and (if not used directly) stored in a -80°C freezer.

Once removed, the plate containing the sorted cells was put on ice for one minute to thaw. RNA-Clean XP beads -used to purify the RNA- were brought to room temperature by removing them from the fridge (4°C) and placing them on a workbench for 30 minutes. Then, 10 µl of nuclease-free water was added to each well of the single-sorted cells.

All experimental steps were conducted under a ventilated hood used explicitly for this purpose. Islam et al. and Trombetta et al. have previously described the reverse transcription methodology used in this study (Islam et al., 2014; Trombetta et al., 2014).

RNA-Clean XP beads were vortexed thoroughly and added to the 96-well plate (33 µl of beads for each well) containing the sorted single cells. The plate was incubated at room temperature for 10 minutes, placed on a magnetic plate and incubated for 5 minutes. Meanwhile, 40 ml of 80 % ethanol was prepared. The supernatant was removed using a 200 µl pipette. Care was taken to ensure that only the supernatant was removed and not the RNA bound to the beads by pipetting opposite the side, where the beads were stuck to the magnetic plate. 125 µl of 80 % ethanol was added to each well. The plate was taken off the magnetic plate and placed on the adjacent row of the magnetic plate.

Consequently, the beads must migrate through the ethanol to the opposite side of the well. Four times, the plate containing the B cells and beads was shifted on the magnetic plate from row to row. The supernatant was removed using a 200 µl pipette. The washing step was then repeated three times. After the last removal of ethanol using a 200 µl pipette, a 20 µl pipette was used to remove all remaining ethanol completely. The plate was air-dried under the hood for 8-10 minutes.

In the meantime, a mix with the following reagents was prepared to elute the RNA from the magnetic beads: random primers (14.5 ng/µl), tergitol, RNase inhibitor (40 U/µl) and nuclease-free water. 11 µl elution mix was added to each well and the beads were resuspended thoroughly. The plate was sealed and incubated in a PCR machine at 65°C for 3 minutes. In the meantime, a second mix for reverse transcription of the RNA was prepared (see Table 5).

PCR Mix - Reverse Transcription	
5X First Strand Buffer	345 µl
Nuclease-free H_2O	235.75 µl
dNTP (25 mM)	57.5 µl
0.1M DTT	115 µl
Rnasin Plus Rnase Inhibitor (40 U/µl)	23 µl
SuperScript	28.75 µl

Table 5 Polymerase Chain Reaction Mix - Reverse Transcription

Then, 7 µl of the reverse transcription mix was added to each well to synthesize cDNA by reverse transcription. Plate was sealed and placed into a PCR machine with the following cycle (see Table 6).

Number of cycles	Temperature	Time
1	42°C	10 min
1	25°C	10 min
1	50°C	60 min
1	94°C	5 min
1	4°C	∞

Table 6 Polymerase Chain Reaction Cycles for Reverse Transcription

10 µl nuclease-free water was added once the PCR cycles were completed. Plates were stored at -20°C or used right away for antibody gene amplification (via nested PCR; subsequently called ‘PCR 1’ and ‘PCR 2’).

2.7 Polymerase Chain Reaction 1

After cDNA synthesis, a 96-well plate contained the cDNA of one cell in each well. The next step was to amplify the genetic region of interest. In this case, it was the IgK and IgH antibody chain locus. The amplification process was done by conducting two PCRs, which will subsequently be called PCR 1 and PCR 2. Both have previously been described by von Boehmer et al. (von Boehmer et al., 2016).

The first PCR (PCR 1) amplifies a larger fragment around the end of the IgK and IgH loci. The second PCR (or PCR 2) amplifies the same fragments but with less overhang from the end of the IgH and IgK loci. This approach yields better sequencing data than just one single PCR. The following table shows the mix for PCR 1 (see Table 7).

PCR Mix for PCR1

Nuclease-free H_2O	3328 µl
10X Buffer	384 µl
dNTP (25 mM)	48 µl
Forward Primer (50 µM)	23 µl
Reverse Primer (50 µM)	15 µl
HotStarTaq DNA Polymerase (250U/50µl)	42 µl

Table 7 Polymerase Chain Reaction Mix for PCR 1

All reagents were pipetted together using a DNA/RNA-free ventilated hood. The mix was prepared in a 15 ml tube and put in a 50 ml pipette basin. 38 µl mix was transferred from the basin to each well of a 96-well PCR plate using a multipipette. All currently unused plates were put on ice when multiple plates were prepared simultaneously. 4 µl of cDNA product was added to each respective well. Therefore, the total volume in a single well was 42 µl. The PCR plate was sealed using adhesive foil, carried to the PCR machine on ice and run with the following program (see Table 8).

Number of cycles	Temperature	Time
1	95°C	15 min
50	94°C	30 sec
	46°C	30 sec
	72°C	55 sec
1	72°C	10 min
1	4°C	∞

Table 8 Polymerase Chain Reaction Cycles for PCR 1

2.8 Loading Buffer

A solution containing 40 grams of sucrose and 100 ml of nuclease-free water was prepared. A few grains of Cresol Red were added.

2.9 Polymerase Chain Reaction 2

PCR 2 is the second PCR performed after cDNA synthesis and amplifies the product of PCR 1 closer to the actual loci of light and heavy chains. After PCR 2, an agarose gel was run to check for IgK and heavy chain bands. If bands were detectable, the plates were sent off for sequencing. If no bands were visible on the gel after having completed PCR 2, both PCR 1 and PCR 2 were repeated. When repeating, the reason for starting with PCR 1 is the inability to check if it is faulty in an efficient way. Running an agarose gel with PCR 1 products shows no bands even when the product is fine. It was therefore decided to be more time efficient to redo both PCRs if no bands were detectable in the agarose gel after PCR 2. The following PCR mix was used for PCR 2 (see Table 9).

PCR Mix for PCR2

Nuclease-free H_2O	2536 µl
Loading Buffer	800 µl
10X Buffer	384 µl
dNTP (25 mM)	48 µl
Forward Primer (50 µM)	15 µl
Reverse Primer (50 µM)	15 µl
HotStarTaq DNA Polymerase (250U/50µl)	42 µl

Table 9 Polymerase Chain Reaction Mix for PCR 2

Like PCR 1, the mix was prepared in a DNA/RNA-free ventilated hood. 38 µl mix was pipetted in each well of the PCR 2 plate. 4 µl of PCR 1 product were added to each respective well of the PCR 2 plate. The PCR plate was sealed using adhesive foil and carried to the PCR machine on ice. The PCR 2 program for light chains is equivalent to PCR 1. The PCR 2 program for heavy chains is as follows (see Table 10).

Number of cycles	Temperature	Time
1	95°C	15 min
50	94°C	30 sec
	55°C	30 sec
	72°C	55 sec
1	72°C	10 min
1	4°C	∞

Table 10 Polymerase Chain Reaction Cycles for PCR 2 - Heavy Chain

For further details, see Viant et al., 2021 and von Boehmer et al., 2016.

2.10 Agarose Gel

1-2 % agarose gels were used to visualize PCR 2 products. Gel red was utilized as a DNA-intercalating agent.

2.11 RNA Sequencing

Illumina's Nextera XT DNA Library Preparation Kit was used to prepare multiplexed sequencing libraries. At Rockefeller University's Genomics Core, libraries were sequenced using an Illumina NovaSeq 6000. An index was created from the Ensembl mouse assembly GRCm38.p5 to pseudo-align the sequence reads using an in-house pipeline. The RNA-seq data files for these analyses have been deposited in the Gene Expression Omnibus of the National Center for Biotechnology Information (accession number GSE174394).

2.12 Use of Software

Biorender was used to create figures, Grammarly to check grammar and provide stylistic writing suggestions, Chat GPT 4.0 to upload relevant literature and ask questions for a better understanding, Prism to create figures and perform statistical analysis, IgBlast to process and align sequences and FlowJo to analyze data. No pre-formulated texts from Chat GPT 4.0 were included in this work.

3. Results

Disclaimer: The majority of experiments in this study have been performed as a group effort by the author of this work and Charlotte Viant with help from the other coauthors. All coauthors participated in experiments and retrospectively, it is not possible to provide an exact allocation of work effort for each experiment to the individual coauthor. The majority of experiments in this study have, however, been conducted by Tobias Wirthmiller and Charlotte Viant as reflected in the author position of the associated paper, showing C. Viant as the first and T. Wirthmiller as the second author. Both T. Wirthmiller and C. Viant discussed the study design and analysis frequently with each other and during lab meetings. Still, credit must be given to Charlotte Viant and Michel Nussenzweig for the originality of the study design and formal analysis. Victor Ramos and Thiago Y. Oliveira contributed to the formal analysis of the data. Mohamed A. ElTanbouly, Spencer T. Chen and Melissa Cipolla performed experiments. Leonidas Stamatatos provided TM4-Core. The data shown in this work has been published prior in the Journal of Experimental Medicine under Charlotte Viant, Tobias Wirthmiller, Mohamed A. ElTanbouly, Spencer T. Chen, Melissa Cipolla, Victor Ramos, Thiago Y. Oliveira, Leonidas Stamatatos, Michel C. Nussenzweig; Germinal center–dependent and –independent memory B cells produced throughout the immune response. *J Exp Med* 2 August 2021; 218 (8): e20202489. DOI: https://doi.org/10.1084/jem.20202489. If not specified otherwise, figures in this thesis have been created by T. Wirthmiller based on the data published in the aforementioned study.

3.1 Transgenic Marker System

An analysis of MBCs requires a system that reliably discriminates them from other B cells. There are several challenges in distinguishing subsets of B cells in flow cytometry. No cell surface markers (e.g., CD38, GL7, etc.) can be used in flow cytometry to determine the number of times a cell has divided. This information is relevant as cells in the GC are thought to divide at a much higher rate than outside, resulting in the number of cell divisions being an indicator of a cell having spent time in the GC. The need for a cell division indicator can be seen for differentiating MBCs that have entered the GC and thus likely divided a lot (GC-dependent MBCs) from MBCs that have not divided rapidly and therefore likely not joined a GC (GC-independent MBCs).

Another challenge is distinguishing follicular B cells from MBCs that have not spent time in the GC, as both are $CD38^{+}$ and $GL7^{-}$.

To address these issues, we generated a double reporter mouse line that allows marking B cell lineages (activated B-, GC cells and their progeny). Methodologically, the lineage-tracking is facilitated through a tamoxifen-inducible Cre recombinase and tetracycline-controlled transcriptional activation system. The creation of the mouse line is based on a sphingosine-1-phosphate receptor 2 Cre recombinase estrogen receptor T2 ($S1pr2^{CreERT2}$) mouse (Shinnakasu et al., 2016), a Rosa26 Zoanthus sp. green fluorescent protein ($R26^{ZsGreen}$) mouse (Madisen et al., 2010) and a H2B-mCherry reporter (Vav^{Tg} $Col1a^{m-Cherry}$) mouse (Gitlin et al., 2014). By breeding these mice together, we created $S1pr2^{CreERT2/+}$ $R26^{ZsGreen/+}$ Vav^{Tg} $Col1a^{mCherry/+}$ mice. A simplified breeding scheme can be seen in Figure 4.

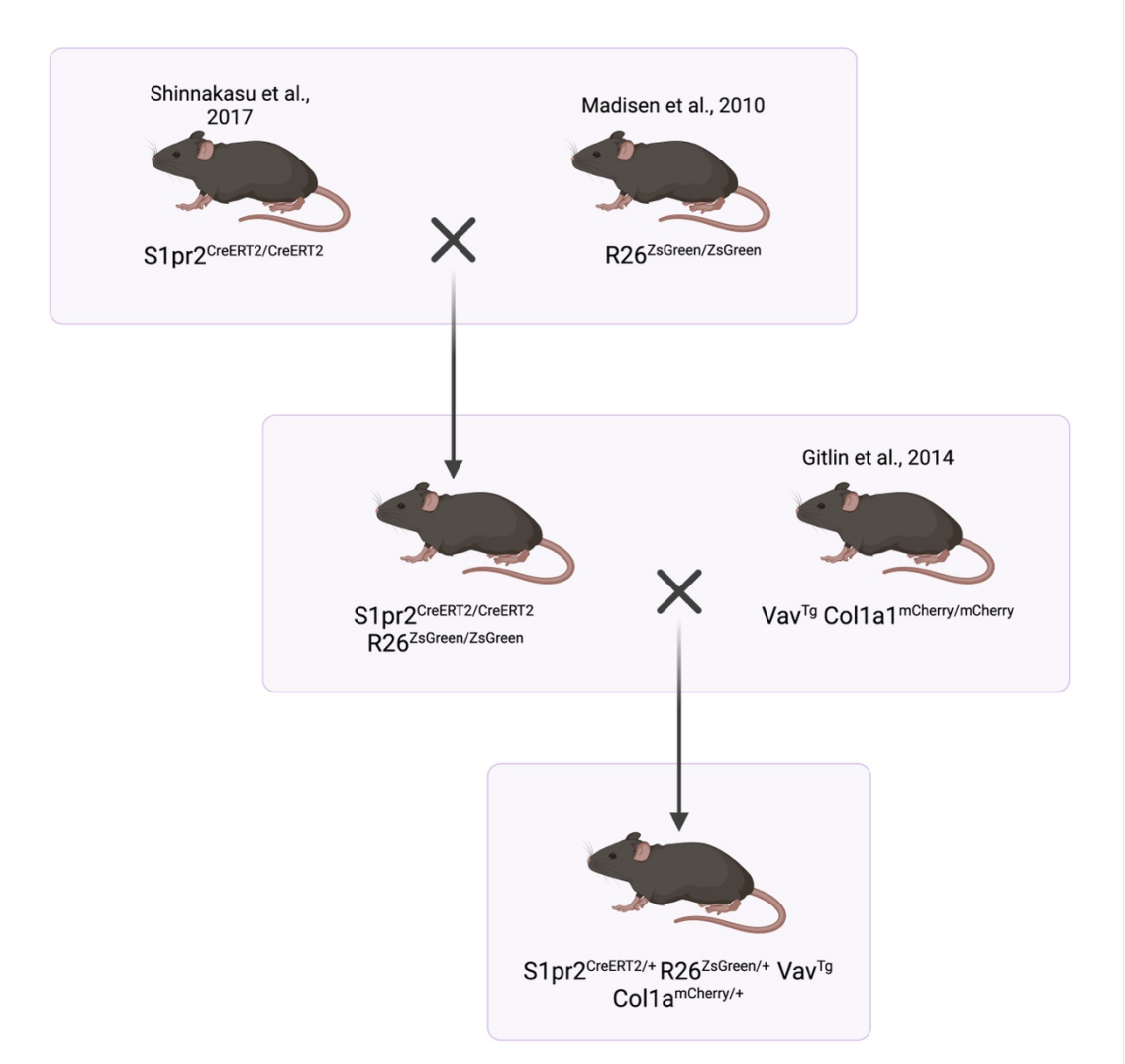

Figure 4 Breeding Scheme for $S1pr2^{CreERT2/+}$ $R26^{ZsGreen/+}$ Vav^{Tg} $Col1a^{mCherry/+}$ Mice: In the first step, $S1pr2^{CreERT2/CreERT2}$ mice (Shinnakasu et al., 2016) were crossed with $R26^{ZsGreen/ZsGreen}$ mice (Madisen et al., 2010) to create $S1pr2^{CreERT2/CreERT2}$ $R26^{ZsGreen/ZsGreen}$ mice. In the second step, $S1pr2^{CreERT2/CreERT2}$ $R26^{ZsGreen/ZsGreen}$ mice were crossed with Vav^{Tg} $Col1a^{mCherry/mCherry}$ mice to create $S1pr2^{CreERT2/+}$ $R26^{ZsGreen/+}$ Vav^{Tg} $Col1a^{mCherry/+}$ mice. Figure created with Biorender.com.

3.1.1 ZsGreen Reporter

The S1pr2^{CreERT2} R26^{ZsGreen} mice are created by crossing S1pr2^{CreERT2} and R26^{ZsGreen} mice. The S1pr2^{CreERT2} mice act as a Cre driver line, whereas R26^{ZsGreen} mice act as a responder line. The responder R26^{ZsGreen} mice line harbors a strong CAG promoter inserted into the Rosa26 locus followed by a stop cassette flanked by loxP sites and the fluorescent marker ZsGreen (Madisen et al., 2010). S1pr2^{CreERT2} R26^{ZsGreen} mice use a tamoxifen-inducible Cre recombinase system to conditionally express the fluorescent protein ZsGreen in S1pr2-controlled cells upon TAM administration (Figure 7).

TAM administration results in the expression of Cre recombinase, which is under the control of an estrogen receptor and the S1pr2 promoter. Cre recombinase activity leads to the removal of the stop cassette at the loxP sites and the expression of ZsGreen. Importantly, Cre (and therefore ZsGreen expression) will only be active in cells expressing S1pr2 (activated B cells, GC cells and their progeny) but not in FBCs (Figure 5).

Therefore, ZsGreen expression can be controlled temporally (upon TAM administration) and spatially (only S1pr2 expressing cells). It enabled us to distinguish FBCs from MBCs as both are CD38^{+} and GL7^{-}, but only MBCs will have expressed S1pr2 and, therefore, be ZsGreen positive. While Figure 5 shows MBCs to express a relatively low amount of S1pr2, it is of importance to note that any progeny of a cell that had previously expressed S1pr2 and been exposed to TAM, will stay ZsGreen positive, disregarding a lower S1pr2 expression at a later time point.

The efficiency of ZsGreen expression was tested by immunizing mice on day 0 with TM4 Core, administering TAM on day 3 by oral gavage and sacrificing mice on day 12 to analyze the lymph nodes (Figure 6). The data shows that approximately 73% of GC cells are marked by ZsGreen after TAM administration.

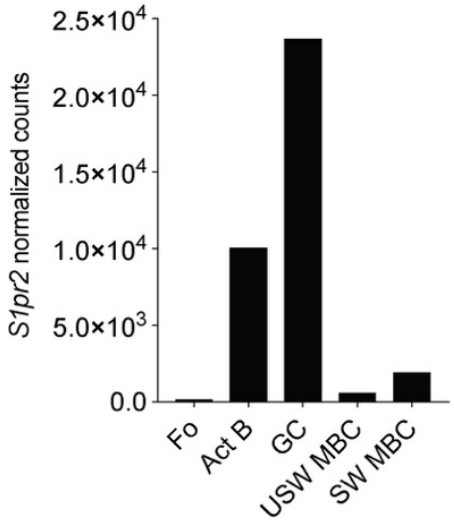

Figure 5 S1pr2 Expression in B Cells: Based on RNA-seq data, the figure displays the level of expression of S1pr2 in follicular (Fo) B cells, activated B cells (Act B), GC cells, unswitched memory B cells (USW MBC) and switched MBCs (SW MBC). Reprinted from Viant et al., 2021 and licensed under CC BY 4.0.

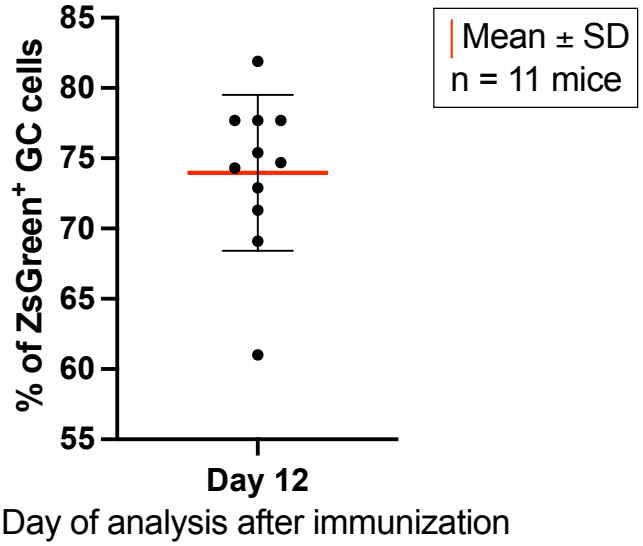

Figure 6 Efficiency of the ZsGreen Reporter System: The figure shows the percentage of positive GC cells for ZsGreen. Mice were immunized on day 0 with TM4-Core, administered with TAM on day 3 and lymph nodes analyzed on day 12. Data are representative of three independent experiments. One dot represents the lymph nodes pooled from one mouse. The bar in red displays the mean +/- the standard deviation.

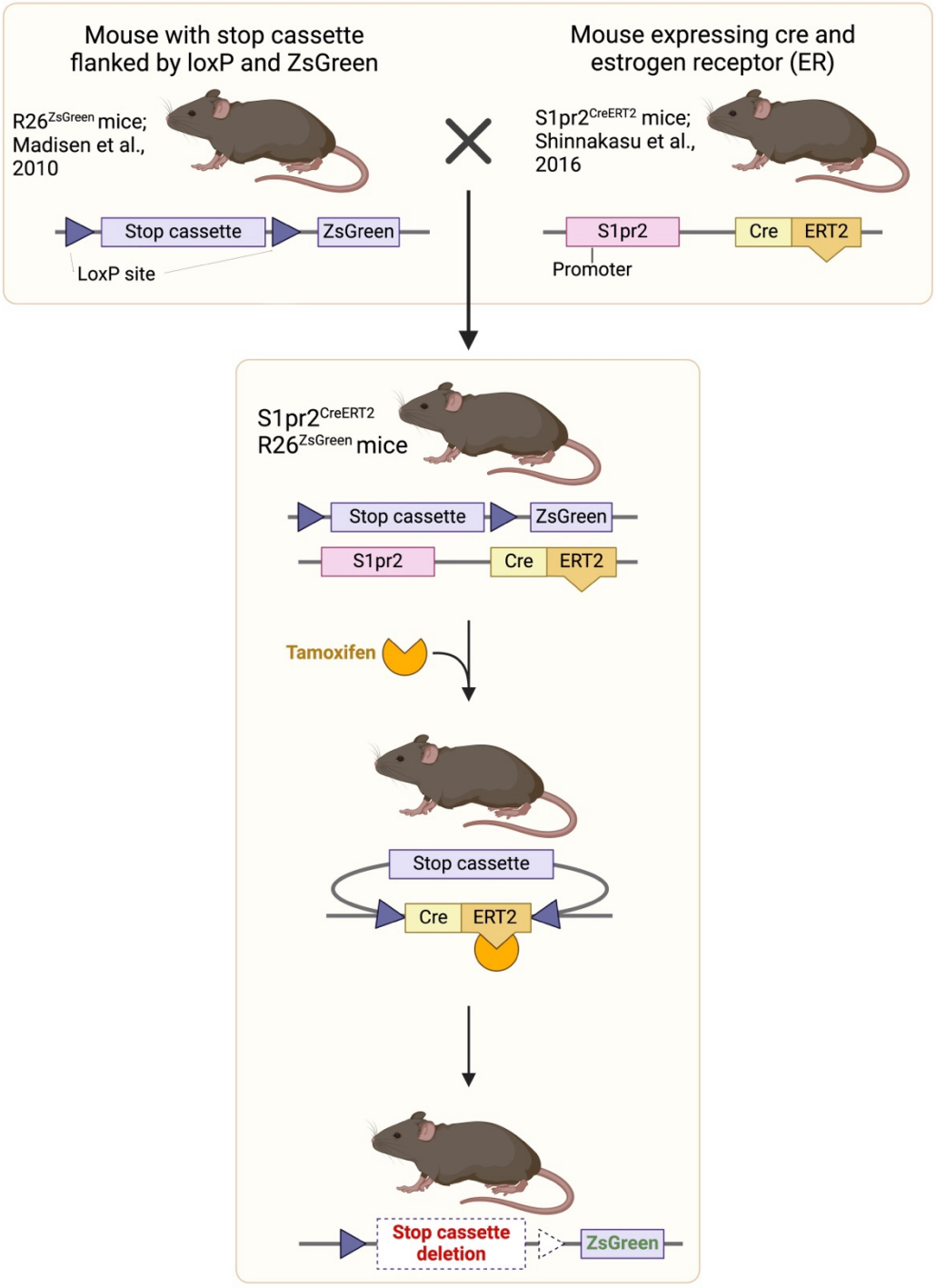

Figure 7 Schematic Representation of the Cre-loxP System in S1pr2^{CreERT2} R26^{ZsGreen} Mice: The figure shows the creation of S1pr2^{CreERT2} R26^{ZsGreen} mice by crossing R26^{ZsGreen} mice (Madisen et al., 2010) with S1pr2^{CreERT2} mice (Shinnakasu et al., 2016). R26^{ZsGreen} mice harbor the fluorescent ZsGreen marker preceded by a stop cassette flanked by loxP sites. S1pr2^{CreERT2} mice harbor an estrogen-controlled Cre recombinase regulated by the S1pr2 promoter. Administration of tamoxifen in S1pr2^{CreERT2} R26^{ZsGreen} mice results in Cre recombinase expression. Cre facilitates the removal of the stop cassette at the loxP sites, resulting in the expression of ZsGreen. Figure created with Biorender.com.

3.1.2 mCherry Reporter

The Vav^{Tg} Col1a mCherry$^{/+}$ mice use a tetracycline-controlled transcriptional activation system to conditionally dilute the mCherry signal in hematopoietic cells upon DOX administration (Figure 8). The expression of mCherry is controlled by the Vav promoter and tetracycline operator (TetO) sequences. The TetO sequences control expression from the collagen type 1, alpha 1 (Col1a1) promoter. Vav is a gene expressed in all hematopoietic cells (Adams et al., 1992; Bustelo et al., 1993; Coppola et al., 1991; Katzav, 2015; Katzav et al., 1989; Ogilvy et al., 1998). Without doxycycline present, a tetracycline transactivator (tTA) protein will bind the DNA at specific TetO sequences in cells with the Vav promoter and result in the expression of mCherry. When DOX is administered, it binds to the tTA, which prevents it from binding to TetO sequences. This ceases mCherry expression. The mCherry signal is fused to the histone H2B, keeping the reporter in the cell's nucleus. Any further division of the cell after doxycycline administration will dilute the mCherry signal in proportion to the number of cell divisions.

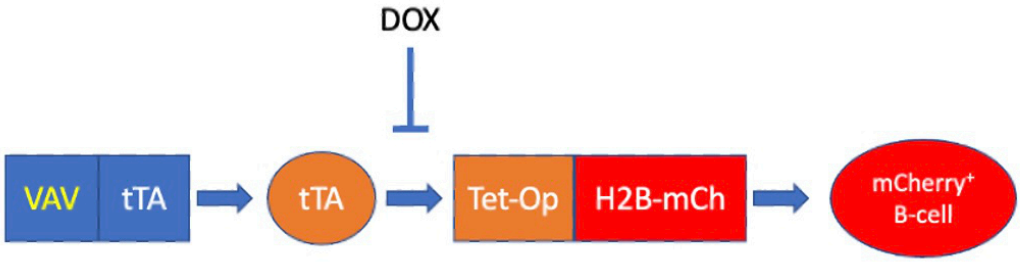

Figure 8 Schematic Representation of the mCherry Reporter Mouse: Doxycycline binds to the tetracycline transactivator element (tTA), thus preventing H2B-mCherry from being expressed in hematopoietic cells carrying the VAV promoter. Figure modified from Viant et al., 2021 and licensed under CC BY 4.0.

Using the proliferation marker CellTrace^{TM} Violet (CTV), cell division was monitored to evaluate the exact number of cell divisions necessary for the mCherry signal to be diluted. We removed B cells from CD45.2 Vav^{Tg} Col1a mCherry$^{/+}$ mice, stained them with CTV *ex vivo* and reinserted them into CD45.1 host mice (Figure 9).

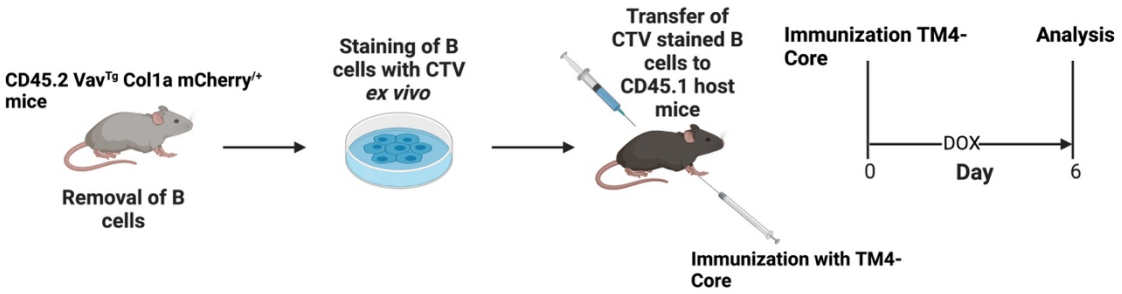

Figure 9 Cell Transfer Protocol for CTV-stained B Cells: B cells were removed from CD45.2 Vav^{Tg} Col1amCherry$^{/+}$ mice, stained *ex vivo* with CTV and transferred to CD45.1 host mice. Host mice were immunized on the same day as cell transfer with TM4-Core and given DOX for 6 days. After six days mice were terminated and analysis was performed by flow cytometry. Figure created with Biorender.com.

The host mice were immunized with the antigen TM4-Core on the same day and given doxycycline for 6 days. Terminating mice took place six days after immunization and B cells were analyzed by flow cytometry. The CTV staining experiment shows that most mCherry^{+} cells did not divide but remained mCherry^{+} up to four divisions. In contrast, mCherry^{-} cells were found to have divided at least four times, with the majority of cells having divided more than eight times (Figure 10). This experiment concludes that mCherry^{+} cells divide no more than four times while mCherry^{-} cells divide at least four times and more.

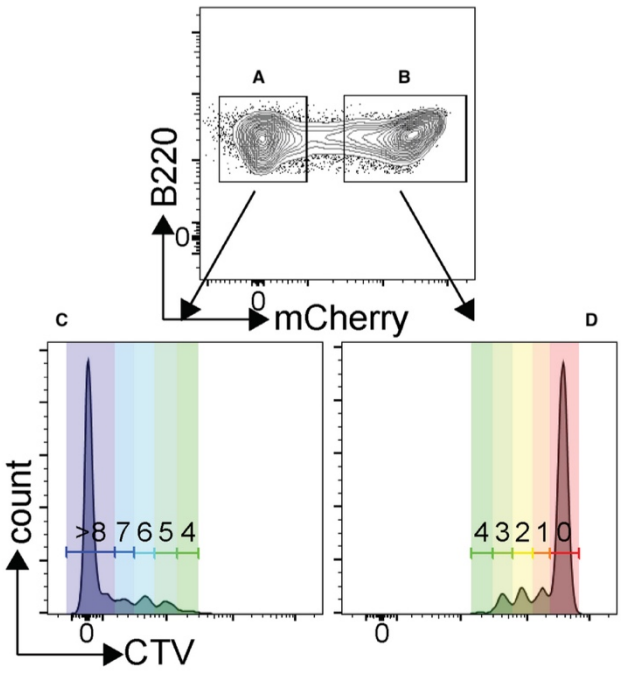

Figure 10 CellTrace^{TM} Violet Cell Transfer Experiment: The flow chart shows mCherry^{-} (**A**) and mCherry^{+} (**B**) MBCs. CTV staining shows that mCherry^{-} MBCs have

divided more than 4 times (**C**) and mCherry^{+} MBCs have divided between 0 and 4 times (**D**). The experimental setup is shown in Figure 9. Data from three independent experiments. Figure modified from Viant et al., 2021 and licensed under CC BY 4.0.

Hence, H2B-mCherry (Vav^{Tg} Col1a1$^{mCherry/+}$) reporter mice mark hematopoietic cells with a red fluorescent protein that allows to estimate whether a cell has likely spent significant time in the GC based on its number of divisions.

3.2 Expression of mCherry in Different Types of B Cells After DOX/TAM Administration

To confirm our findings with CTV as a proliferation marker, we performed an experiment demonstrating mCherry expression in different B cells 12 days after immunization. Figure 11 shows the experimental setup: day 0 marks the immunization with the HIV Ag TM4-Core. On day 6, the mice are treated with DOX for six days. This results in the binding of DOX to the tTA, which stops the expression of mCherry and initiates its dilution. The timeframe of six days of DOX administration was chosen to make sure that B cells that divide often have sufficient time to dilute the mCherry signal. From day 9 to day 12, mice are treated with TAM. On day 12, mice were sacrificed. As the mice were treated with TAM from day 9 to day 12, S1pr2 expressing cells were marked with ZsGreen during this timeframe.

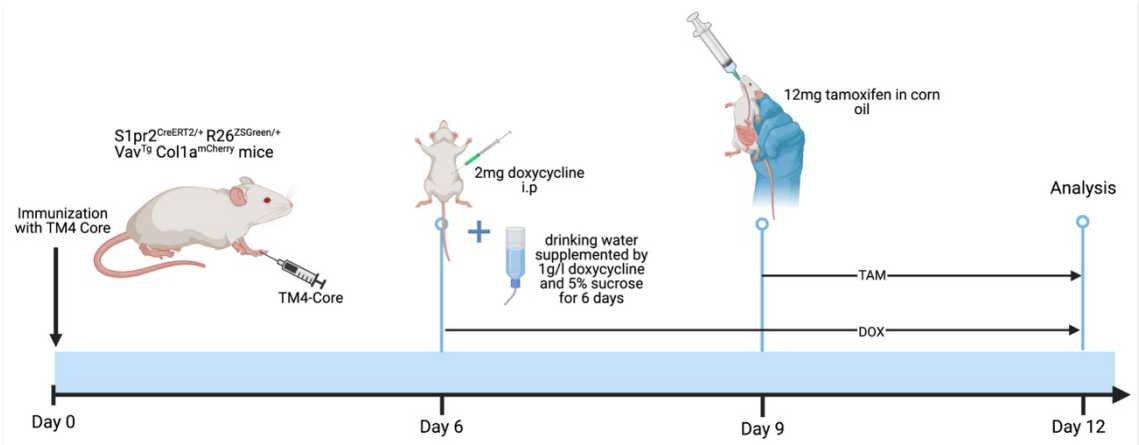

Figure 11 Experimental Setup of Immunization and DOX/TAM Administration for Day 12: Mice are immunized with the HIV-antigen TM4-Core (footpad injection) on day 0. Doxycycline (2 mg) was administered to mice by i.p injection on day 6. The drinking water was supplemented by 1g/l doxycycline and 5 % sucrose for 6 days (days 6 to 12). On day 9, tamoxifen (12 mg) diluted in corn oil was given to mice by oral gavage. Mice were terminated by CO_2 overdoses for analysis on day 12. Figure created with Biorender.com.

Figure 12 shows that follicular B cells do not dilute the mCherry signal, as more than 99 % of cells are mCherry$^+$. While Figure 5 shows some S1pr2 expression, no follicular B cells express ZsGreen (Figure 12). GC cells completely dilute the mCherry signal and are mCherry$^-$. Most activated B cells divide no more than four times, with only a small number dividing more frequently as shown in the experiments with CTV (Figure 10). Therefore, the majority of activated B cells are mCherry$^+$. Another population of activated B cells with an IgD$^-$ phenotype was not further considered in this study as this cell group appears already in the GC pathway (Hägglöf et al., 2023; Viant et al., 2021). MBCs do not show a strong tendency to adapt to one mCherry behavior fully. Approximately half of the MBCs are mCherry$^-$ and half are mCherry$^+$ (Figures 12 and 13).

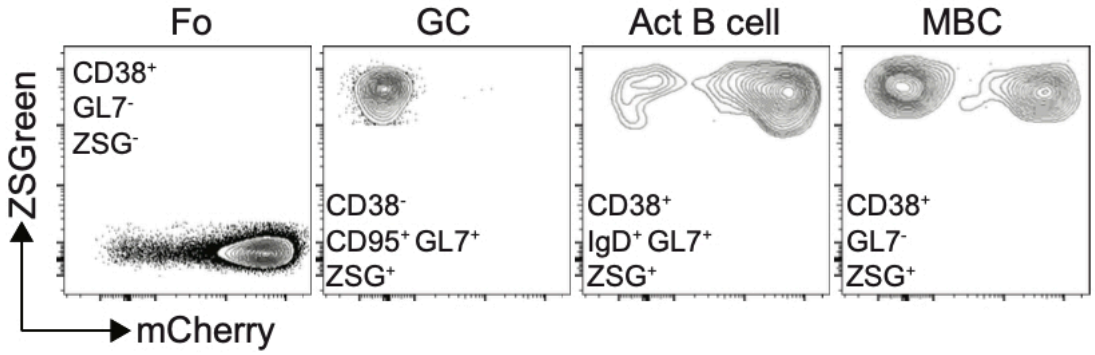

Figure 12 ZsGreen and mCherry Reporter Expression in B Cells: The flow chart shows the expression of mCherry and ZsGreen in follicular (Fo), GC, activated B (Act B) and MBCs after TAM/DOX administration (see Figure 11 for experimental setup). Figure is reprinted from Viant et al., 2021 and licensed under CC BY 4.0.

With half the MBC population harboring a mCherry$^+$ signal, it is likely that these cells did not enter the GC and, thus, must have originated independently.

These experiments demonstrate that our transgenic marker system successfully marks GC cells, activated and follicular B cells and GC-dependent and -independent MBCs.

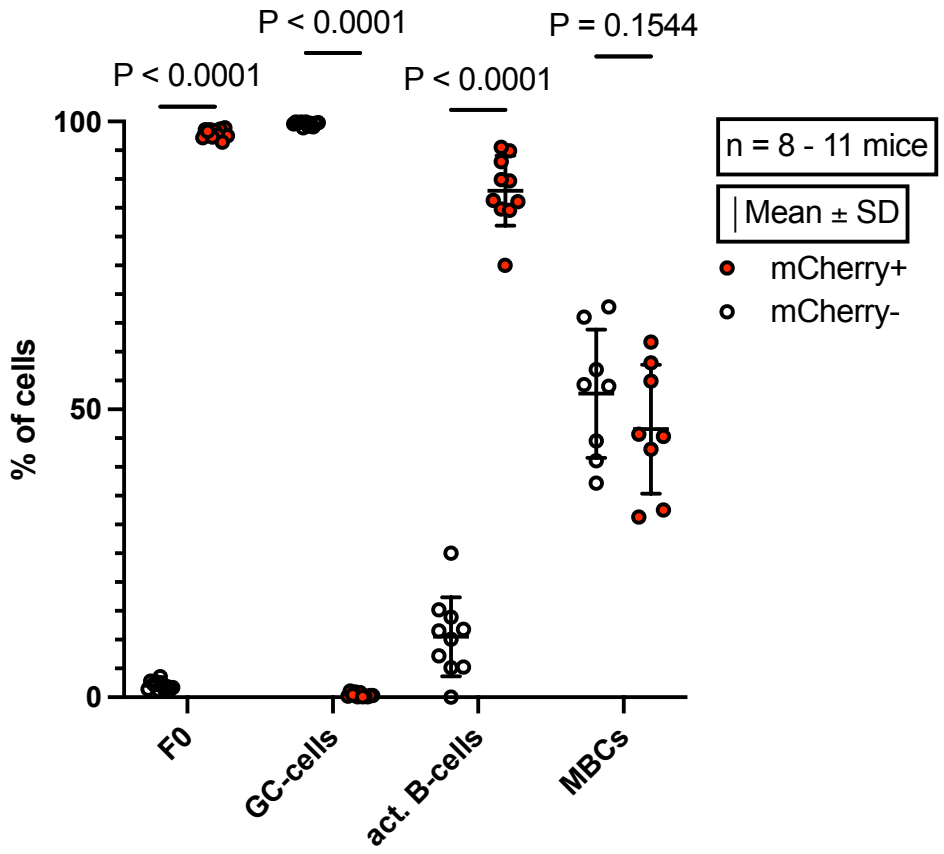

Figure 13 Expression of mCherry in B Cells after DOX Administration: The figure shows the expression of the mCherry signal in follicular B cells (F0), GC cells, activated B cells (act. B cells) and MBCs after DOX administration (see Figure 11 for experimental setup). Each dot represents data from the lymph nodes of one mouse. Data shown are from three independent experiments and 11 mice in total. Some of the groups (e.g. MBCs) show data from less than 11 mice as the experiments did not work for all mice in these groups. Analysis by two-way ANOVA. Data previously published by Viant et al., 2021.

3.3 MBCs Are Perpetually Generated Outside of the GC

As reported in the Introduction of this thesis, several authors had previously noticed that MBCs can originate from a GC-independent pathway. So far, however, GC-independent MBCs have only been observed in mice with no GC formation (Kaji et al., 2012; Taylor et al., 2012; Toyama et al., 2002) or for a very limited time before the formation of a GC (Weisel et al., 2016).

The previous experiment demonstrated the production of GC-independent MBCs in mice that can form a GC. However, it is vital to determine whether GC-independent MBC production can only be observed before GC formation or constantly during the immune reaction.

To investigate this question, we performed an experiment that analyzed the production of MBCs after immunization at three different time points for ten days using the transgenic mouse model described above.

Transgenic mice were immunized with TM4-Core at day 0 and sacrificed on days 19, 25 and 31 to analyze the production of MBCs throughout the GC reaction. In group 1, DOX was administered 6 days post-immunization until day 12. Six days of DOX administration were chosen to ensure a complete dilution of the mCherry signal among GC cells. Mice were treated with TAM from day 9 to day 19 (Figure 14).

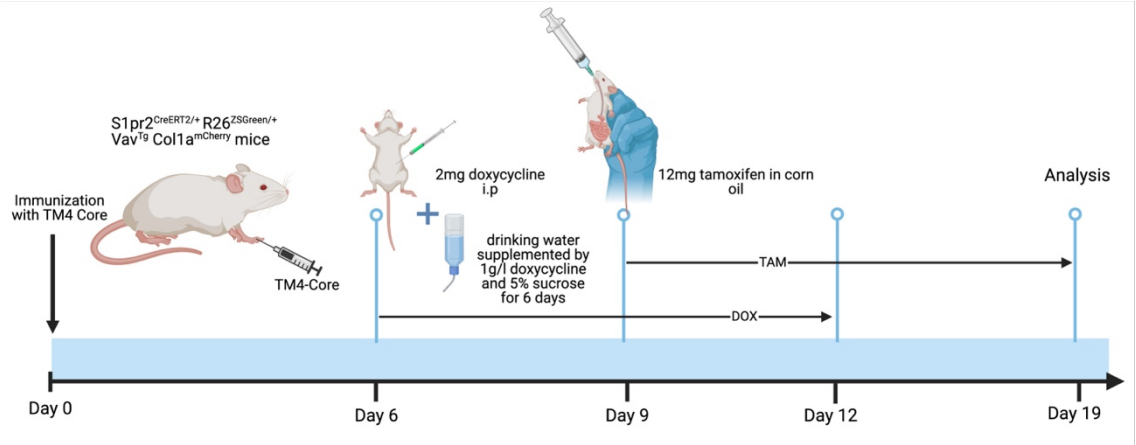

Figure 14 Experimental Setup of Immunization and DOX/TAM Administration for Day 19: Mice are immunized with the HIV-antigen TM4-Core (footpad injection) on day 0. Doxycycline (2 mg) was administered to mice by i.p injection on day 6. The drinking water was supplemented by 1g/l doxycycline and 5 % sucrose for 6 days (days 6 to 12). On day 9, tamoxifen (12 mg) diluted in corn oil was given to mice by oral gavage. Mice were terminated by CO_2 overdoses for analysis on day 19. Figure created with Biorender.com.

In group 2, DOX was given from day 12 to day 18 and TAM was given from day 15 to day 25 (Figure 15).

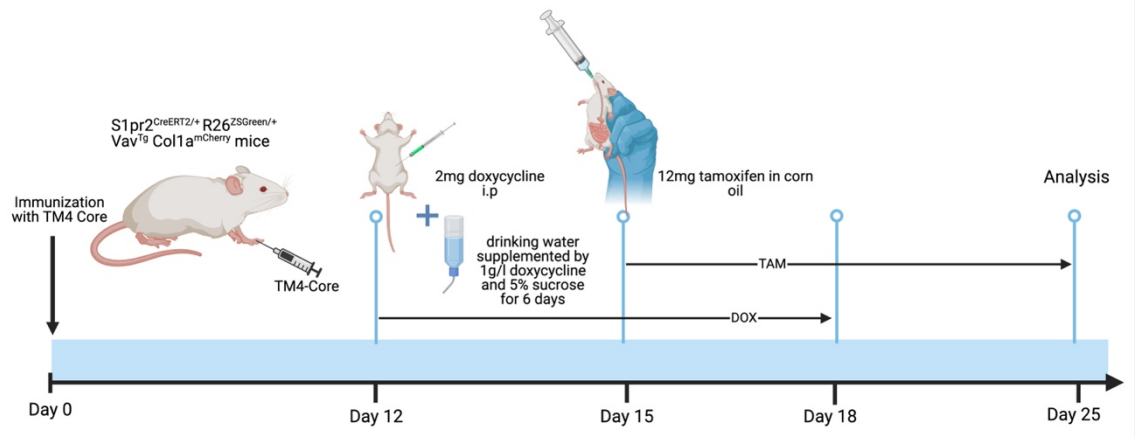

Figure 15 Experimental Setup of Immunization and DOX/TAM Administration for Day 25: Mice are immunized with the HIV-antigen TM4-Core (footpad injection) on day

0. Doxycycline (2 mg) was administered to mice by i.p injection on day 12. The drinking water was supplemented by 1g/l doxycycline and 5 % sucrose for 6 days (days 12 to 18). On day 15, tamoxifen (12 mg) diluted in corn oil was given to mice by oral gavage. Mice were terminated by CO_2 overdoses for analysis on day 25. Figure created with Biorender.com.

In group 3, DOX was given from day 18 to day 24 and TAM was given from day 21 to day 31 (Figure 16).

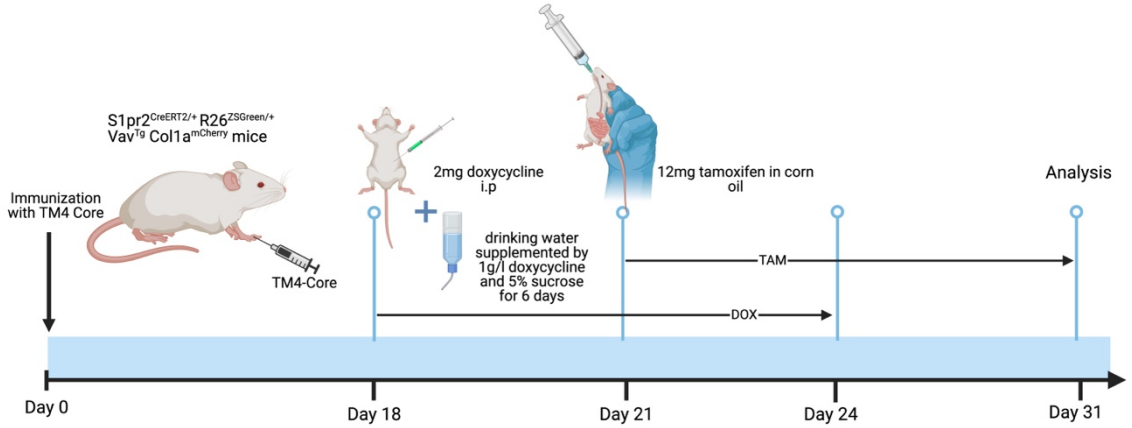

Figure 16 Experimental Setup of Immunization and DOX/TAM Administration for Day 31: Mice are immunized with the HIV-antigen TM4-Core (footpad injection) on day 0. Doxycycline (2 mg) was administered to mice by i.p injection on day 18. The drinking water was supplemented by 1g/l doxycycline and 5 % sucrose for 6 days (days 18 to 24). On day 21, tamoxifen (12 mg) diluted in corn oil was given to mice by oral gavage. Mice were terminated by CO_2 overdoses for analysis on day 31. Figure created with Biorender.com.

This allowed for analysis of MBC production over ten days at three different time points in the GC reaction (Figure 17).

Figures 17 and 18 show two populations of MBCs: mCherry$^-$ and mCherry$^+$ MBCs. Both populations are produced constantly during the immune reaction. Figure 19 shows that the absolute counts of mCherry$^+$ MBCs, collected from lymph nodes of one mouse, vary between 102 and 1339 cells and for mCherry$^-$ MBCs between 299 and 2765 cells.

Figures 17, 18 and 19 visualize that mCherry$^+$ MBCs are constantly produced from day 9-19, day 15-25 and day 21-31. The results indicate that GC-independent MBCs are continuously made throughout the GC reaction in mice that can form a GC. These findings consolidate the model that two distinct MBC subtypes exist and that GC-independent MBCs are not simply an unphysiological reaction in mice missing a GC.

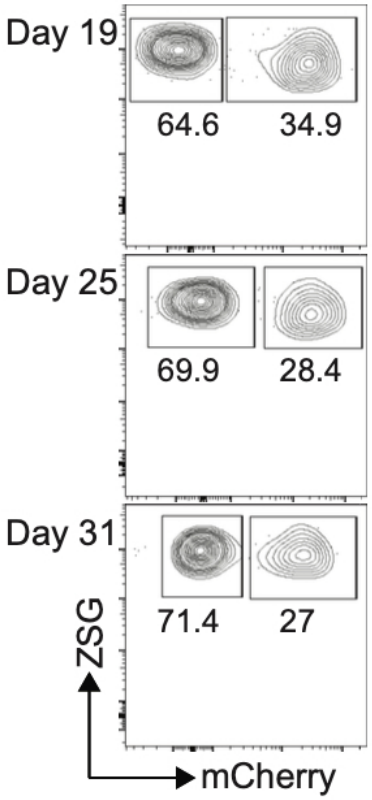

Figure 17 Two MBC Subsets: This figure shows the flow chart of two different MBC populations continuously produced during the immune reaction. The MBC populations differ in their mCherry signal ($mCherry^+$ and $mCherry^-$ MBCs). Reprinted from Viant et al., 2021 and licensed under CC BY 4.0.

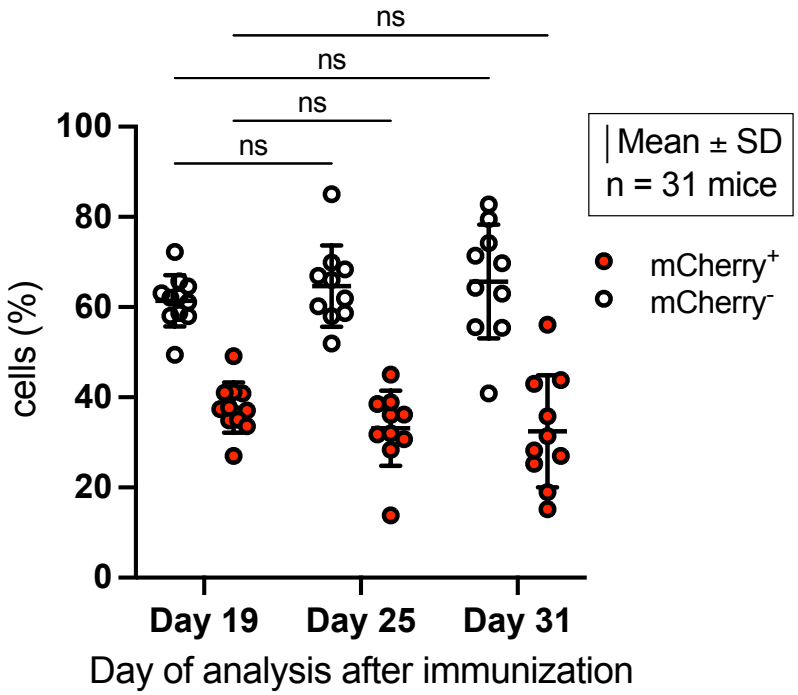

Figure 18 Continuous Production of GC-independent and -dependent MBCs During the Immune Reaction: The figure shows the percentage of $mCherry^-$ and $mCherry^+$ MBCs produced at three different time points in the immune reaction (Day 9 to 19, Day

15 to 25 and Day 21 to 31). The data represents three independent experiments and was analyzed by two-way ANOVA. Each dot represents one mouse. Between 10 – 11 mice were used for each time point and 31 mice in total. Data previously published by Viant et al., 2021.

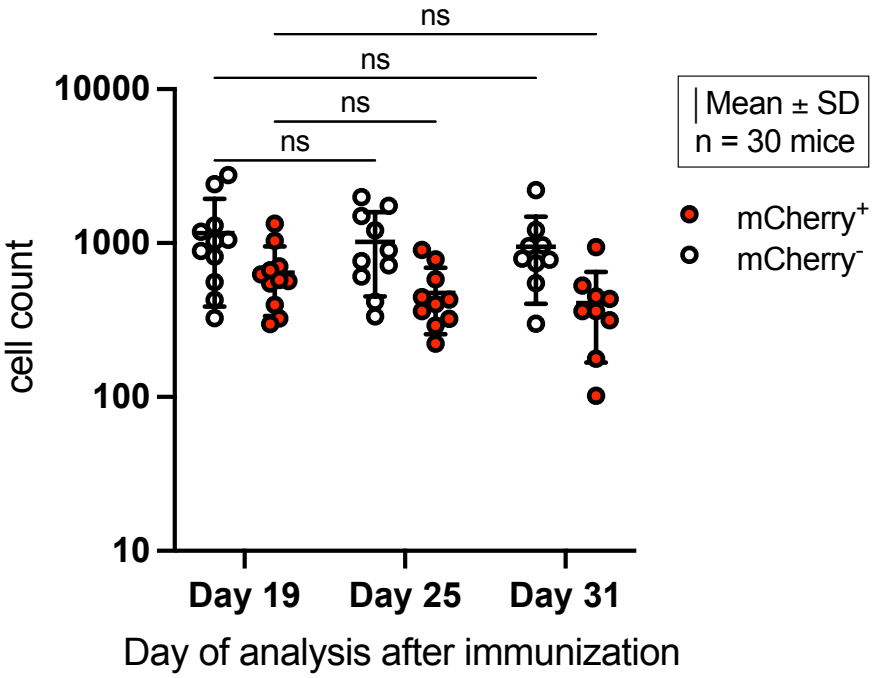

Figure 19 Absolute Counts of mCherry$^-$ and mCherry$^+$ MBCs: The figure shows the absolute cell counts of mCherry$^-$ and mCherry$^+$ MBCs produced at three different time points in the immune reaction (Day 9 to 19, Day 15 to 25 and Day 21 to 31). The data represents three independent experiments and was analyzed by two-way ANOVA. Each dot represents one mouse. Between 9 – 11 mice were used for each time point and 30 mice in total. Data previously published by Viant et al., 2021.

3.4 GC-dependent MBCs Contain Switched and Unswitched Isotypes; GC-independent MBCs Are Almost Exclusively Unswitched

Having obtained more evidence supporting a model comprising two sets of MBCs, GC-dependent and -independent, we wanted to understand how they differ and, ideally, draw conclusions about differences in functionality. To this end, we performed an experiment looking at the switching behavior of MBCs.

To analyze the BCR isotype among mCherry$^+$ and mCherry$^-$ MBCs, double reporter mice treated with DOX and TAM (analogous to the experimental setup in Figures 14, 15 and 16) were terminated at day 19, day 25 and day 31 and cells were analyzed by flow cytometry. This setup of experiments allowed us to compare the percentage of switched MBCs in the respective MBC departments.

Figures 20 and 21 show the percentage of IgM$^-$ IgD$^-$ MBCs among mCherry$^+$ and mCherry$^-$ MBC populations. The mCherry$^+$ MBC population contains only a small number of switched MBCs at Day 19 and 25, making them an almost exclusively isotype-unswitched population. This contrasts the mCherry$^-$ MBC population, which harbors switched and unswitched MBCs. These results demonstrate that GC-independent MBCs are predominantly of the same isotype class (IgM$^+$ IgD$^+$).

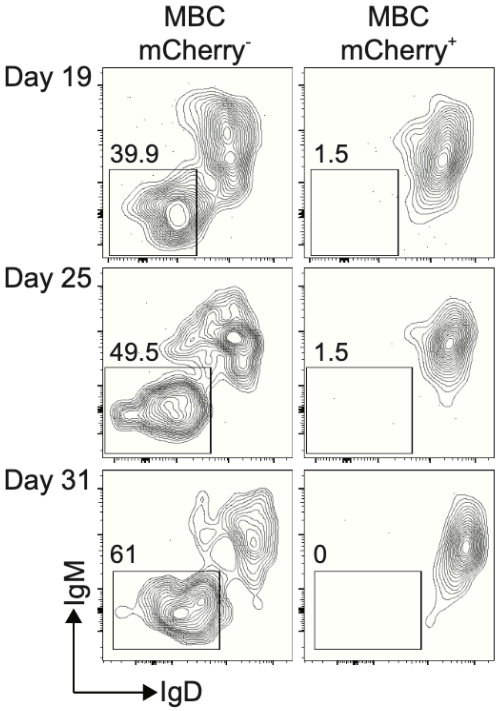

Figure 20 Flow-cytometry Analysis of MBC Isotypes: The figure shows that mCherry$^+$ MBCs are almost exclusively unswitched (IgM$^+$ IgD$^+$), whereas mCherry$^-$ MBCs are partly switched (IgM$^-$ IgD$^-$) and unswitched (IgM$^+$ IgD$^+$). Reprinted from Viant et al., 2021 and licensed under CC BY 4.0.

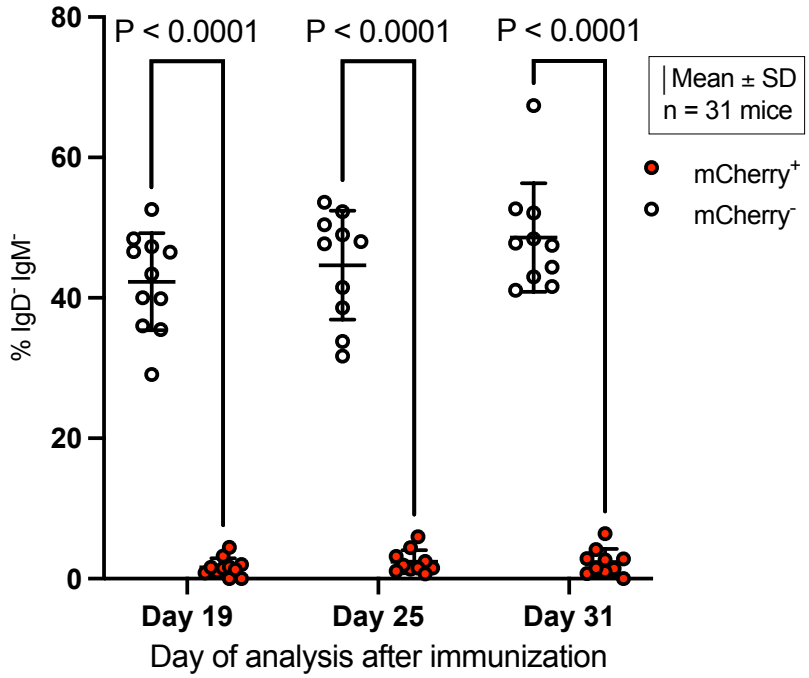

Figure 21 Isotype Class of MBCs: The figure shows the percentage of IgD$^-$ IgM$^-$ MBCs among the mCherry$^+$ and mCherry$^-$ MBC populations at three different time points from the lymph nodes of 31 mice. Each dot represents one mouse. The data shows 10 – 11 mice for each time point and 31 mice in total. The data represent three independent experiments (Days 19, 25 and 31). P-value < 0.0001, two-way ANOVA. Data previously published by Viant et al., 2021.

3.5 GC-dependent MBCs Have a Higher Number of Mutations Than GC-independent MBCs

Another indicator suggesting GC-dependent MBCs have spent time within the GC is their accumulated number of mutations in their heavy and light chain genes. Due to their time spent in the GC undergoing SHMs, GC-dependent MBCs are expected to have more mutations than GC-independent MBCs. To test this hypothesis, we used fluorescence-activated cell sorting (FACS) to sort single MBCs, reverse transcribed the mRNA into cDNA, performed a nested PCR, sequenced the PCR amplicons and analyzed the number of mutations by aligning the sequencing results of the antibody genes to a germline reference.

Figure 22 shows the number of heavy and light chain mutations from mCherry$^+$ and mCherry$^-$ MBCs and demonstrates that GC-dependent MBCs have a higher mean of mutations (5) than GC-independent MBCs (mean of 2 mutations). The observation about the mean of mutations is very similar at all three time points analyzed. This further supports the idea that mCherry$^-$ MBCs originate from the GC, as cells are unlikely to obtain such high numbers of mutations elsewhere in the LN. Interestingly, a few cells among both compartments show very high numbers of mutations.

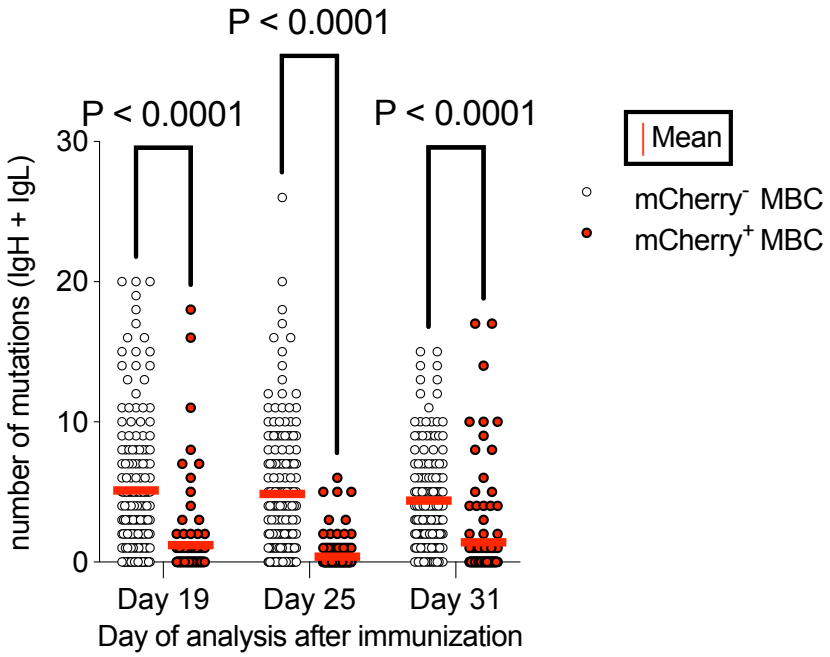

Figure 22 Mutations in MBCs: Number of heavy and light chain mutations in mCherry$^-$ and mCherry$^+$ MBCs. This figure shows that mCherry$^-$ MBCs have a higher mean of mutations than mCherry$^+$ MBCs. P-value < 0.0001, two-way ANOVA. The red bar indicates the mean. Each dot shows the number of mutations (nucleotides) from IgH and IgL within the antibody genes sequenced of one MBC. The data represents three independent experiments and n = 7-15 mice were used for each group (Day 19, 25 and 31). Data previously published by Viant et al., 2021.

3.6 MBCs Do Not Originate From Prominent GC B Cell Clones

Our understanding of the selection process inside the GC still needs to be improved. More research is required to understand the exact mechanisms influencing a GC cell to become an MBC or a PC (see Introduction). To further understand the selection procedure of MBCs inside the GC, we investigated the clonality of GC-dependent MBCs, GC-independent MBCs and GC cells.

A clone was defined as sharing a heavy chain or a heavy and a light chain. We used FACS to sort single MBCs and GC cells, reverse transcribed the mRNA into cDNA, performed a nested PCR, sequenced the PCR amplicons and analyzed the clonality of single cells. Figures 23, 24 and 25 show the data for three experiments conducted on day 19, day 25 and day 31. At day 19 post-immunization, three murine LNs were sorted and single-cell sequencing was performed. The same procedure was repeated with mice for day 25 and day 31. The experimental setup is shown in Figures 14, 15 and 16.

Figure 23 shows a common heavy chain (IgH) between clone 5 of GC cells and clone 1 of mCherry$^-$ MBCs on Day 19 and a shared heavy and light chain (IgL) between clone 1

of GC cells and clone 1 of mCherry$^-$ MBCs on Day 31. Figure 24 demonstrates no clonality is shared between MBCs and GCs in lymph node 2. Figure 25 shows a shared heavy and light chain between clone 1 of GC cells and clone 1 of mCherry$^-$ MBCs on Day 19. Furthermore, clone 2 of GC cells and clone 1 of mCherry$^+$ MBCs on Day 19 share a common IgH. Clone 6 of GC cells shares a common IgH and IgL with clone 1 of mCherry$^-$ MBCs on Day 31. Altogether, only five clones are shared between the GC cell clones and MBCs. These results demonstrate that GC cells form dominant clones. However, MBCs primarily do not originate from these clones but from single cells (singlets) that do not form large clonal families. This provides evidence that MBCs arise from a diverse set of precursor cells.

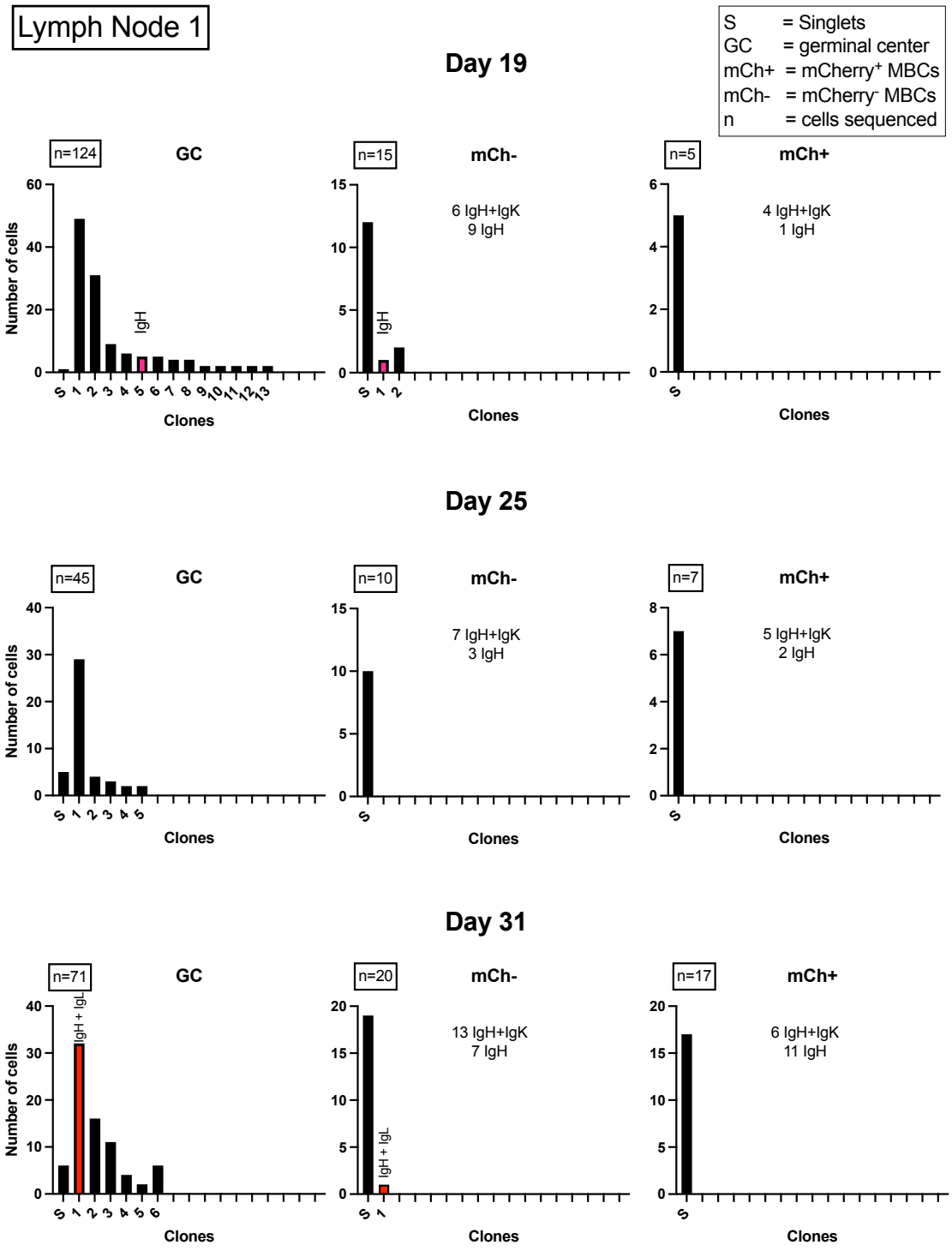

Figure 23 Lymph Node 1. Clonality of GC Cells, mCherry$^-$ and mCherry$^+$ MBCs: This figure shows a common IgH between clone 5 of GC cells and clone 1 of mCherry$^-$ MBCs on Day 19. Furthermore, a shared IgH and IgL can be seen between clone 1 of GC cells and clone 1 of mCherry$^-$ MBCs on Day 31. Clone = Common IgH + IgL chain or common IgH chain. Data previously published by Viant et al., 2021

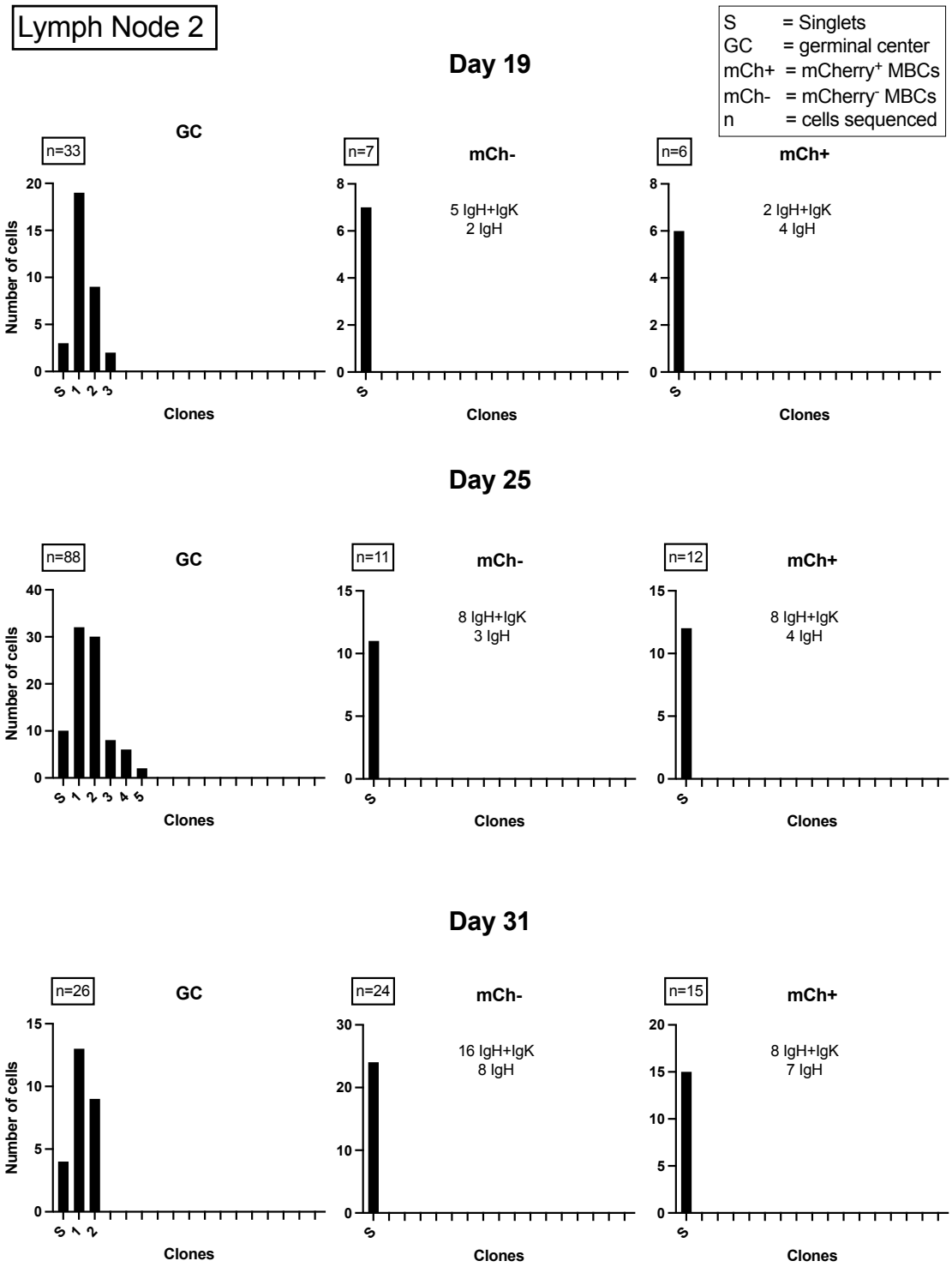

Figure 24 Lymph Node 2. Clonality of GC Cells, mCherry$^-$ and mCherry$^+$ MBCs: In lymph node 2, no common clones were found between MBCs and GC cells. Clone = Common IgH + IgL chain or common IgH chain. Data previously published by Viant et al., 2021.

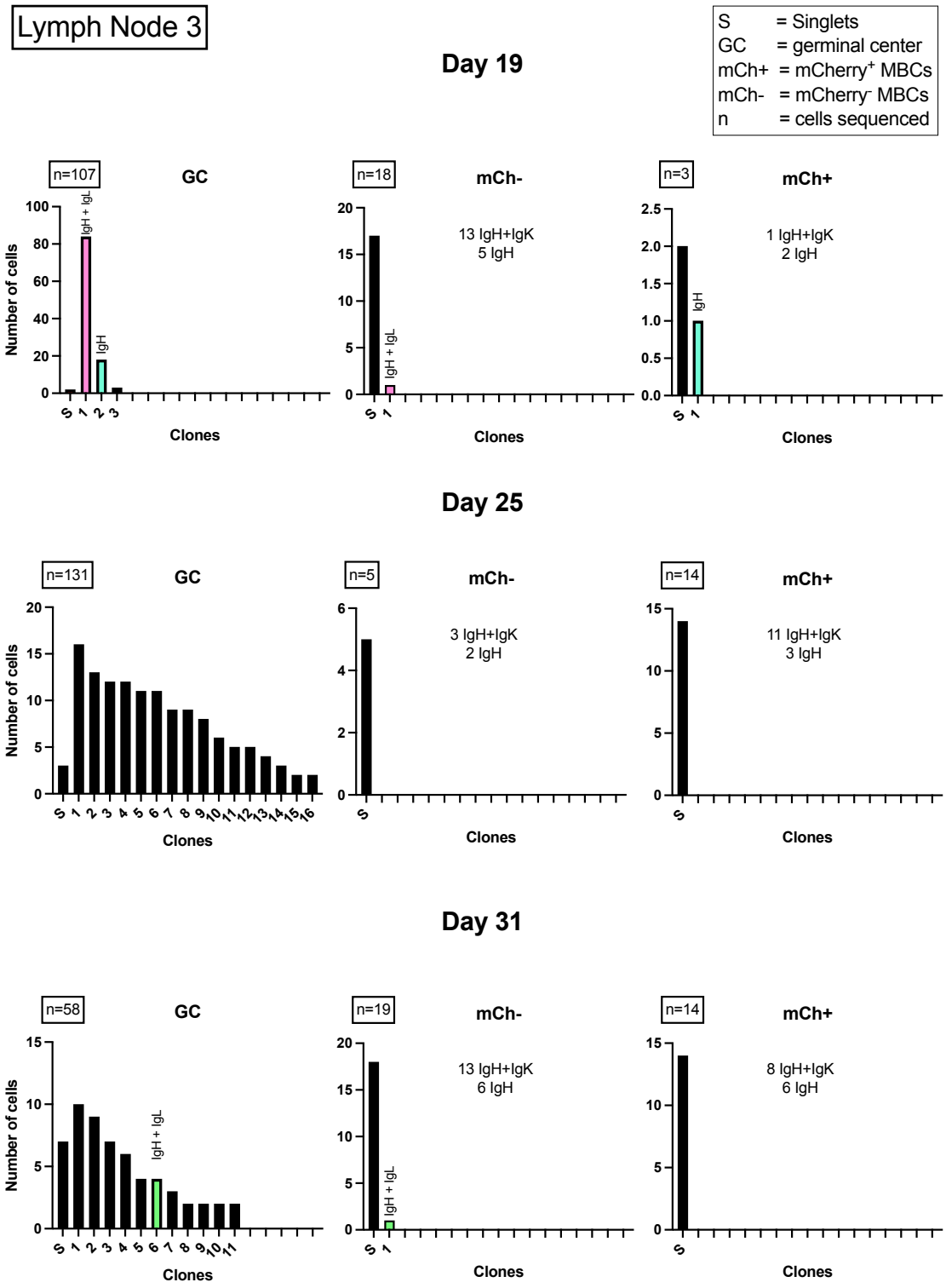

Figure 25 Lymph Node 3. Clonality of GC Cells, mCherry- and mCherry+ MBCs: This figure shows a shared IgH and IgL chain between clone 1 of GC cells and clone 1 of mCherry- MBCs on Day 19. Furthermore, clone 2 of GC cells and clone 1 of mCherry+ MBCs on Day 19 share a common IgH. Clone 6 of GC cells shares a common IgH and IgL with clone 1 of mCherry- MBCs on Day 31. Clone = Common IgH + IgL chain or common IgH chain. Data previously published by Viant et al., 2021.

4. Discussion

4.1 Lineage-Tracking System

As Akkaya et al. pointed out, the old Romans knew that somebody who had gotten the plague once would not get sick a second time (Akkaya et al., 2020). This is only partially true for all diseases. Still, infection with a disease often results in long-lasting immunity mediated by long-lived PCs and MBCs. The discovery of the GC and its product cells, PCs and MBCs, have contributed immensely to our current understanding of immunity. With more and more research in this field, concepts are constantly challenged and re-thought. Initially only thought to originate from the GC, several authors have demonstrated the existence of GC-independent MBCs (Kaji et al., 2012; Matsumoto et al., 1996; Taylor et al., 2012; Toyama et al., 2002; Weisel et al., 2016).

In this study, we were particularly interested in whether this second population of MBCs can be attributed to the lack of an intact immune system (such as Bcl6 -/- mice) or could also be observed in a physiological mouse with a functioning immune system for more extended periods than those before GCs formed. To that objective, we used an unbiased lineage-tracking system involving a ZsGreen Cre/loxP recombination system and a mCherry dilution reporter to follow the formation of MBCs within an intact murine immune system. This thesis aimed to assess the existence and properties of GC-independent MBCs during physiological immune responses. In addition, through flow cytometry analysis and single-cell RNA sequencing, we strived to improve the understanding of the mechanisms underlying immunological processes by comparing MBC subsets and other B cells.

The data shows that the ZsGreen-mCherry tracking system is reliable for tracking B cell lineages based on cell divisions and S1pr2 expression. Flow cytometry analysis shows two different MBC populations in mice harboring a physiological immune system. Furthermore, the GC-independent MBC population was shown to be continuously produced for at least 30 days after immunization and to exhibit fewer mutations in their antibody genes and switched isotypes than the GC-dependent population. The data further suggests that both MBC populations arise from singlets rather than prominent B cell clones.

Several authors have previously demonstrated the existence of GC-independent MBCs (Kaji et al., 2012; Matsumoto et al., 1996; Taylor et al., 2012; Toyama et al., 2002; Weisel et al., 2016). Many of these studies, however, were conducted in mice with an impaired immune system. Matsumoto et al. utilized LTα -/- mice that cannot form a GC in their

studies (Matsumoto et al., 1996). According to Toyama et al., LTα -/- mice do not provide excellent conditions for studying MBCs due to the poor IgG antibody responses observed in these mice upon immunization with sheep red blood cells (Fu et al., 1997; Toyama et al., 2002) and the unfavorable microenvironment impairing the activation of memory responses (Fu et al., 2000). Similar to this, Blr1-deficient mice used by Förster et al. have morphologically altered primary lymphoid follicles due to impaired lymphocyte migration into splenic follicles (Förster et al., 1996; Toyama et al., 2002). Toyoma et al. used Bcl6 -/- RM mice that were created by transferring bone marrow cells of Bcl6-deficient mice into RAG1 -/- mice (Fukuda et al., 1997; Toyama et al., 2002) because Bcl6-deficient mice alone suffered from growth retardation and mostly died at a young age (Toyama et al., 2002). These mice can express histologically normal marginal zones, periarterial lymphoid sheaths and primary B cell follicles in the spleen. However, as Kaji et al. pointed out (Kaji et al., 2012), Bcl6 germline deletions can affect the immune system negatively by causing arrested T follicular helper cells (Crotty, 2011), impaired DC development (Ohtsuka et al., 2011) and aberrant macrophage functions (Mondal et al., 2010). A Bcl6 germline deletion also causes a prominent inflammatory disease by overproducing T helper cell cytokines (Dent et al., 1997; Ye et al., 1997) and changing the properties of B cells before immunization (Shaffer et al., 2000). Kaji et al., therefore, utilized a conditional Bcl6 deletion model and no change was observed in the number, phenotype, or cytokine production of B cells after stimulation through the BCR (Kaji et al., 2012). However, these mice still lack a GC, raising the question of whether the production of GC-independent MBCs is merely an unphysiological reaction to the absence of a GC.

Studies showing GC-independent MBCs in mice that can form a GC have only demonstrated their production for a limited time during the immune response (Kaji et al., 2012; Weisel et al., 2016). MBCs observed before GC formation are GC-independent. It is, however, challenging to distinguish GC-independent MBCs from GC-dependent MBCs once a GC has been formed. Therefore, previous studies could have been cautious in assessing the production of MBCs in mice with an intact immune system once the GC has formed. This could be due to the lack of suitable cell surface markers to distinguish GC-dependent from GC-independent MBCs. CD73 was previously suggested as a marker to separate GC-dependent from GC-independent MBCs (Taylor et al., 2012) but discarded as it was neither exclusive nor specific for GC-dependent MBCs (Weisel et al.,

2016). Another challenge lies in distinguishing between naïve B cells and MBCs, which are both $CD38^{+}$ $GL7^{-}$ (Taylor et al., 2012).

The B cell lineage-tracking system used in this work circumvents these challenges as it can distinguish between GC-dependent and GC-independent MBCs by the expression of mCherry. GC-dependent MBCs usually divide more than four times and dilute the mCherry signal. Furthermore, it can separate naïve B cells and MBCs by the expression of S1pr2 and subsequent marking with ZsGreen. This allows tracking GC-dependent and GC-independent MBCs along the immune response without the need for cell surface receptors.

The experiment with CTV also demonstrates why the mCherry system is a more convenient way of marking B cells than using dyes such as CTV. Using dyes has two disadvantages: 1. The cells must be removed, stained *ex vivo* and reinjected into the new mouse and 2. not all cells in the new mouse will be marked, only the reinjected B cells.

Additionally, former studies (Kaji et al., 2012; Pape et al., 2011; Taylor et al., 2012; Toyama et al., 2002) investigating MBCs only looked at MBCs with high affinity to an Ag (e.g. Phycoerythrin (PE) or 4-Hydroxy-3-nitrophenylacetyl hapten conjugated to Chicken Gamma Globulin (NP-CGG)) bound to a fluorescent marker. In the experiments of Pape et al., mice had about one in 5000 and one in 25,000 PE- and allophycocyanin-specific B cells, respectively. About 20,000 B cells were specific for PE in the naive B cell pool (Pape et al., 2011). Similarly, in other studies, PE-specific B cells make up 0.057% (Unenriched) or 4% (PE enriched) of B cells (Taylor et al., 2012). Fluorescent marker systems that require antigen-specific MBCs fail to consider many MBCs with lower affinity because they cannot bind to the antigen-fluorescent marker complex. Furthermore, some studies gate only for IgG MBCs, leaving out cells from a different BCR class (Suan et al., 2017). The lineage-tracking system in this work does not rely on antigen-specific B cells nor restrictions in gating for IgG MBCs, thus allowing a more significant number of B cells, including those with lower affinity to an antigen, to be considered in the analysis.

One of the most exciting discoveries of this work is the observation of the continuous production of GC-independent MBCs during the immune response in mice with an intact immune system. In previous studies, it was a common conception that GC-independent MBCs would arise early after immunization and are later joined by MBCs originating from the GC reaction (Kaji et al., 2012; Taylor et al., 2012; Weisel et al., 2016). A potential reason why we observed the production of GC-independent MBCs later in the GC

reaction, unlike the previous studies, could be the higher number of MBCs analyzed altogether (see Figure 19) through our lineage-tracking system, including low-affinity MBCs. Therefore, GC-independent MBC production may have also been present later in previous studies but not captured in the analysis. Furthermore, a lack of appropriate markers to distinguish GC-dependent from GC-independent MBCs could have made it more difficult to differentiate between GC-dependent and GC-independent MBCs after GC formation.

4.2 Isotype Expression of Memory B Cell Subsets

Until now, MBCs expressing IgM, IgG, IgA and IgE isotypes have been observed (Kurosaki et al., 2015). Isotype expression of MBCs is often tied to their role and functionality in immune responses. In our study, we found the mCherry$^-$ (GC-dependent) population to contain a much higher amount of switched MBCs, whereas the mCherry$^+$ population (GC-independent) was almost exclusively unswitched. This remains mostly the same throughout the entire GC reaction. The mCherry$^-$ population (GC-dependent MBCs) appears less homogenous in their BCR expression. Around half of them are switched, whereas the other half is unswitched. Interestingly, there is a slight trend among mCherry$^+$ cells towards the switched isotype from day 19 to day 31 during the GC reaction. Generally, these findings concur with data from prior publications relevant to this topic (Taylor et al., 2012; Toyama et al., 2002; Weisel et al., 2016). Taylor et al. observed that most IgM MBCs and early switched MBCs were GC-independent and later switched MBCs GC-dependent (Taylor et al., 2012). Similarly, Weisel et al. found that MBCs created before the GC reaction were mostly IgM$^+$, although some IgG MBCs were also produced during day 0 to day 2 after immunization (Weisel et al., 2016). While these studies show that IgM and IgG MBCs can be created in a GC-independent fashion, there is evidence that IgM MBCs can outnumber IgG MBCs (Pape et al., 2011). While we could observe a small number of switched GC-independent MBCs (see Figures 20 and 21), most GC-independent MBCs were IgM$^+$. Therefore, we can confirm the tendency of GC-independent MBCs to be IgM$^+$ as seen in prior studies. Furthermore, while IgM$^+$ MBCs can arise from both GC-dependent and GC-independent origins, IgG MBCs appear to originate mainly from a GC-dependent origin.

4.3 Mutations in Memory B Cells and Selection Process in the Germinal Center

The number of mutations observed in MBCs in this work supports the abovementioned conclusions: GC-dependent MBCs had a higher mean number of mutations in their antibody genes (namely 5) than GC-independent MBCs (mean of 2 mutations). This is not surprising as cells in the GC undergo SHMs, obtaining a higher number of mutations. Several papers showed a lack of mutations in GC-independent B cells with Bcl6 deficiency (Kaji et al., 2012; Toyama et al., 2002), raising the question of whether this phenomenon can be causally attributed to the absence of Bcl6 in these cells or an inherent inability in GC-independent MBCs to accumulate SHM. Our observations support that the utter lack of mutations is likely due to the Bcl6 deficiency rather than an intrinsic property of GC-independent MBCs. Pape et al. considered most IgM^+ MBCs to be GC-independent and observed a low amount of mutations in these cells (Pape et al., 2011), suggesting they do not express the right amount of activation-induced enzyme required for Ig isotype switching and SHMs (Taylor et al., 2012). However, Dogan et al. described a population of IgM^+ MBCs with a slightly larger number of mutations (between 1 and 27 mutations), namely $CD73^+$ IgM^+ MBCs (Dogan et al., 2009). While $CD73^+$ might not be a suitable marker for distinguishing GC-independent from GC-dependent MBCs (see above), MBCs with somatic mutations appear enriched in the $CD73^+$ subset (Kaji et al., 2012). Our results align with previous data that GC-independent MBCs generally have a lower number of mutations. IgM^+ MBCs with a higher number of mutations, similar to the IgM^+ $CD73^+$ MBC subset observed by Dogan et al., or the PE-specific IgM^+ $CD73^+$ MBCs observed by Taylor et al., could represent the IgM^+ cells originating from the GC (Dogan et al., 2009; Taylor et al., 2012). Another explanation for some of the mutations acquired by GC-independent MBCs could be the expression of activation-induced enzyme in activated B cells before joining a GC (Roco et al., 2019).

Questions remain on the mechanisms behind the selection in the GC for an MBC or a PC fate. There is some evidence that competition between B cells occurs before the GC, with the ‘winners’ dominating the GC reaction.

Schwickert et al. investigated the competition between B cells before joining the GC (Schwickert et al., 2011). An adoptive transfer experiment in mice found competition between high and low-affinity B cells outside the GC, with the higher-affinity clones dominating the GC reaction. High-affinity B cells would capture more Ags and receive

more T cell help mediated by the density of pMHC expressed on the cell surface. All of which led to a higher emergence of high-affinity B cell clones in the GC.

In conclusion, a pre-GC competition among B cell clones is taking place and it is based on affinity and T cell help (Schwickert et al., 2011). The threshold for GC-entry must be low as high-affinity GC B cells can have germline versions with very low affinities to the Ag (Scheid et al., 2009). Our experiments concluded that MBCs originating from the GC arise from singlets. The failure to develop prominent clones within the GC supports the concept that MBCs arise from a diverse set of precursor cells with a lower affinity (Shinnakasu et al., 2016; Suan et al., 2017).

4.4 Functionality of Memory B Cell Subsets in the Immune Response

Regarding functionality, the role of GC-independent and GC-dependent MBCs remains to be discussed. Dogan et al. suggested that IgG MBCs spawn into plasmablasts upon re-activation. In contrast, IgM MBCs join a GC to undergo further affinity maturation and clonal expansion before engaging in the immune response (Dogan et al., 2009). Switched MBCs from the GC are likely to have a high affinity due to mutations in their antibody genes obtained in the GC. This would make them better suited for differentiation into plasmablasts immediately. IgM MBCs, with an assumed lower affinity due to their lower mean number of mutations, would join a GC to increase their affinity before engaging in the immune response. However, it has also been observed that IgM cells can become plasmablasts and switched cells can join a GC (Weisel and Shlomchik, 2017).

Other authors suggest a model where the decision between joining a GC or spawning as a plasmablast is not determined by the BCR isotype but by the expression of cell surface markers (Weisel and Shlomchik, 2017). They organized MBCs in three subsets based on the expression of the cell surface markers CD80 and PD-L2: Double negative (DN) MBCs ($CD80^-$ and $PD\text{-}L2^-$), single positive (SP) MBCs ($CD80^-$ and $PD\text{-}L2^+$) and double positive (DP) MBCs ($CD80^+$ and $PD\text{-}L2^+$). This model shows that DN MBCs join GCs upon re-activation, DP MBCs become plasmablasts and SP MBCs can do either of the two options. Distinction by cell surface marker or BCR isotype do not exclude each other but largely overlap: DN MBCs are primarily comprised of IgM MBCs, DP MBCs are to the extent of approximately 50% made from IgG and SP MBCs are in between the DN and DP proportions (Weisel and Shlomchik, 2017).

Pape et al.'s work supports the tendency observed in prior studies that IgG MBCs can generate plasmablasts and IgM MBCs can create GCs. Additionally, they aimed to provide more information on the mechanisms behind IgM MBCs responses upon Ag rechallenge. They found that switched IgG^+ MBCs increased 150-fold in numbers upon Ag rechallenge, whereas IgM MBCs only increased less than 2-fold. They assumed the poor IgM response was due to functional inhibition by the presence of neutralizing serum Ig. It was found that switched IgG^+ MBCs dominated the secondary response, despite being shorter-lived and outnumbered by IgM^+ MBCs, due to their ability to be activated with highly neutralizing serum Ig present. Switched Ig^+ MBCs appear to generate plasmablasts and memory cells upon rechallenge, but IgM MBCs could act as a reservoir if Ig serum levels decline. Switched Ig^+ MBCs could not form GC in Pape et al.'s experiment. Still, IgM MBCs could create GCs, suggesting that IgM MBCs could be essential in responding to Ag variations originating from mutating pathogens (Pape et al., 2011).

We found GC-independent MBCs to be mainly IgM^+, confirming previous research results. The GC-dependent subset of MBCs is likely closely related to double-positive MBCs ($CD80^+$ and PD-$L2^+$) and GC-independent MBCs could be similar to the double-negative MBCs ($CD80^-$ and PD-$L2^-$). Therefore, GC-independent MBCs likely contribute to the immune response by joining or founding GCs upon Ag rechallenge, possibly once Ig serum levels decline (Pape et al., 2011).

4.5 Limitations of the Study

Interpreting the results requires consideration of a few limitations. Methodologically, our lineage-tracking system cannot prove that $mCherry^-$ cells have entered the GC. Therefore, when referring to GC-dependent MBCs or GC-independent MBCs, it is based on criteria such as the number of mutations a cell has accumulated and the number of divisions a cell has gone through.

In some cases, Cre can create a phenotype alone due to the random integration of the transgene when creating Cre mice. As Shinnakasu et al. created the S1pr2-ERT2cre mice through injection of the transgene into pronuclei of mice zygotes (Shinnakasu et al., 2016), it would theoretically be possible that there are effects through the integration of Cre into a random site ('position effect'), that could have affected our results. While not hemizygous, the heterozygous expression of Cre instead of the homozygous expression could have alleviated possible positioning effects.

Furthermore, Cre-inducible systems could be prone to 'leakiness': there are reported cases of Cre expression in specific tissues without the induction through tamoxifen (Liu et al., 2010). As we studied B cells in the lymph node, the effects of leakiness would probably have affected B cells or cells in the lymph node in general, marking cells ZsGreen without the induction of tamoxifen. As we do not see a distinct expression of ZsGreen in B cells that do not express S1pr2, the effects of leakiness are, if present, most likely neglectable in our study.

Regarding the efficiency of reporter protein expression, the flow cytometry data showed nearly all follicular B cells to be efficiently marked mCherry^{+} and almost all GC cells to be marked mCherry^{-}, demonstrating a highly efficient reporting capacity. Nearly 73% of GC cells are marked by ZsGreen. The efficiency in the ZsGreen reporter system is lower than that in the mCherry system. Still, the double reporter mice are an efficient tool for B cell lineage tracking.

Other limitations include a lack of external validation, as our study does not translate to humans or animals without further research. The results regarding the clonality of MBCs contain a small sample size (n=3 – 24 cells), but it needs to be taken into consideration that MBCs are not a very numerous B cell population to begin with and 10 – 100 MBCs can already generate a relevant antibody response (Weisel and Shlomchik, 2017). Another limitation lies in the lack of studying long-term effects as we did not examine e.g. re-exposure responses to antigens after many months or years.

4.6 Conclusion

In conclusion, we identified two subsets of MBCs in mice harboring a physiological immune system and could show the continuous production of both subsets throughout the immune response. MBCs perform an essential role in the immune response against viral escape mutations (Purtha et al., 2011) and could, therefore, have critical implications for the development of future vaccines. Experiments that include tracking GC-independent MBCs upon re-challenge could lead to a deeper understanding of their functional contribution to the immune response. Further work is required to better understand MBCs, especially how the results discovered in this and other studies translate to humans.

References

Adams, J.M., H. Houston, J. Allen, T. Lints, and R. Harvey. 1992. The hematopoietically expressed vav proto-oncogene shares homology with the dbl GDP-GTP exchange factor, the bcr gene and a yeast gene (CDC24) involved in cytoskeletal organization. *Oncogene*. 7:611–618.

Akkaya, M., K. Kwak, and S.K. Pierce. 2020. B cell memory: building two walls of protection against pathogens. *Nat. Rev. Immunol.* 20:229–238. doi:10.1038/s41577-019-0244-2.

Allman, D., and S. Pillai. 2008. Peripheral B cell subsets. *Curr. Opin. Immunol.* 20:149–157. doi:10.1016/j.coi.2008.03.014.

Anderson, S.M., M.M. Tomayko, A. Ahuja, A.M. Haberman, and M.J. Shlomchik. 2007. New markers for murine memory B cells that define mutated and unmutated subsets. *J. Exp. Med.* 204:2103–2114. doi:10.1084/jem.20062571.

Angeli, V., and G.J. Randolph. 2006. Inflammation, lymphatic function, and dendritic cell migration. *Lymphat. Res. Biol.* 4:217–228. doi:10.1089/lrb.2006.4406.

Baden Lindsey R., El Sahly Hana M., Essink Brandon, Kotloff Karen, Frey Sharon, Novak Rick, Diemert David, Spector Stephen A., Rouphael Nadine, Creech C. Buddy, McGettigan John, Khetan Shishir, Segall Nathan, Solis Joel, Brosz Adam, Fierro Carlos, Schwartz Howard, Neuzil Kathleen, Corey Lawrence, Gilbert Peter, Janes Holly, Follmann Dean, Marovich Mary, Mascola John, Polakowski Laura, Ledgerwood Julie, Graham Barney S., Bennett Hamilton, Pajon Rolando, Knightly Conor, Leav Brett, Deng Weiping, Zhou Honghong, Han Shu, Ivarsson Melanie, Miller Jacqueline, and Zaks Tal. 2021. Efficacy and Safety of the mRNA-1273 SARS-CoV-2 Vaccine. *N. Engl. J. Med.* 384:403–416. doi:10.1056/NEJMoa2035389.

von Behring, E., and S. Kitasato. 1991. The mechanism of diphtheria immunity and tetanus immunity in animals. 1890. *Mol. Immunol.* 28:1317, 1319–1320.

von Boehmer, L., C. Liu, S. Ackerman, A.D. Gitlin, Q. Wang, A. Gazumyan, and M.C. Nussenzweig. 2016. Sequencing and cloning of antigen-specific antibodies from mouse memory B cells. *Nat. Protoc.* 11:1908–1923. doi:10.1038/nprot.2016.102.

Bogoslowski, A., and P. Kubes. 2018. Lymph Nodes: The Unrecognized Barrier against Pathogens. *ACS Infect. Dis.* 4:1158–1161. doi:10.1021/acsinfecdis.8b00111.

Bontumasi, N., J.A. Jacobson, E. Caoili, C. Brandon, S.M. Kim, and D. Jamadar. 2014. Inguinal lymph nodes: size, number, and other characteristics in asymptomatic patients by CT. *Surg. Radiol. Anat.* 36:1051–1055. doi:10.1007/s00276-014-1255-0.

Bryda, E.C. 2013. The Mighty Mouse: The Impact of Rodents on Advances in Biomedical Research. *Mo. Med.* 110:207–211.

Bustelo, X.R., S.D. Rubin, K.L. Suen, D. Carrasco, and M. Barbacid. 1993. Developmental expression of the vav protooncogene. *Cell Growth Differ. Mol. Biol. J. Am. Assoc. Cancer Res.* 4:297–308.

Carrasco, Y.R., and F.D. Batista. 2007. B Cells Acquire Particulate Antigen in a Macrophage-Rich Area at the Boundary between the Follicle and the Subcapsular Sinus of the Lymph Node. *Immunity*. 27:160–171. doi:10.1016/j.immuni.2007.06.007.

Chambers, E.S., and M. Vukmanovic-Stejic. 2020. Skin barrier immunity and ageing. *Immunology*. 160:116–125. doi:10.1111/imm.13152.

Chen, R.E., X. Zhang, J.B. Case, E.S. Winkler, Y. Liu, L.A. VanBlargan, J. Liu, J.M. Errico, X. Xie, N. Suryadevara, P. Gilchuk, S.J. Zost, S. Tahan, L. Droit, J.S. Turner, W. Kim, A.J. Schmitz, M. Thapa, D. Wang, A.C.M. Boon, R.M. Presti, J.A. O'Halloran, A.H.J. Kim, P. Deepak, D. Pinto, D.H. Fremont, J.E. Crowe, D. Corti, H.W. Virgin, A.H. Ellebedy, P.-Y. Shi, and M.S. Diamond. 2021. Resistance of SARS-CoV-2 variants to neutralization by monoclonal and serum-derived polyclonal antibodies. *Nat. Med.* 27:717–726. doi:10.1038/s41591-021-01294-w.

Coffey, F., B. Alabyev, and T. Manser. 2009. Initial Clonal Expansion of Germinal Center B Cells Takes Place at the Perimeter of Follicles. *Immunity*. 30:599–609. doi:10.1016/j.immuni.2009.01.011.

Collin, M., and V. Bigley. 2018. Human dendritic cell subsets: an update. *Immunology*. 154:3–20. doi:10.1111/imm.12888.

Cooper, M.D., R.D.A. Peterson, and R.A. Good. 1965. Delineation of the Thymic and Bursal Lymphoid Systems in the Chicken. *Nature*. 205:143–146. doi:10.1038/205143a0.

Coppola, J., S. Bryant, T. Koda, D. Conway, and M. Barbacid. 1991. Mechanism of activation of the vav protooncogene. *Cell Growth Differ. Mol. Biol. J. Am. Assoc. Cancer Res.* 2:95–105.

Crotty, S. 2011. Follicular Helper CD4 T Cells (T_{FH}). *Annu. Rev. Immunol.* 29:621–663. doi:10.1146/annurev-immunol-031210-101400.

Dagan, N., N. Barda, E. Kepten, O. Miron, S. Perchik, M.A. Katz, M.A. Hernán, M. Lipsitch, B. Reis, and R.D. Balicer. 2021. BNT162b2 mRNA Covid-19 Vaccine in a Nationwide Mass Vaccination Setting. *N. Engl. J. Med.* 384:1412–1423. doi:10.1056/NEJMoa2101765.

Dent, A.L., A.L. Shaffer, X. Yu, D. Allman, and L.M. Staudt. 1997. Control of inflammation, cytokine expression, and germinal center formation by BCL-6. *Science*. 276:589–592. doi:10.1126/science.276.5312.589.

Dogan, I., B. Bertocci, V. Vilmont, F. Delbos, J. Mégret, S. Storck, C.-A. Reynaud, and J.-C. Weill. 2009. Multiple layers of B cell memory with different effector functions. *Nat. Immunol.* 10:1292–1299. doi:10.1038/ni.1814.

Dunn, T.B. 1954. Normal and Pathologic Anatomy of the Reticular Tissue in Laboratory Mice, With a Classification and Discussion of Neoplasms. *JNCI J. Natl. Cancer Inst.* 14:1281–1433. doi:10.1093/jnci/14.6.1281.

Fenner, F., D.A. Henderson, I. Arita, Z. Jezek, I.D. Ladnyi, and W.H. Organization. 1988. Smallpox and its eradication. World Health Organization, Geneva. 1460 pp.

Förster, R., A.E. Mattis, E. Kremmer, E. Wolf, G. Brem, and M. Lipp. 1996. A Putative Chemokine Receptor, BLR1, Directs B Cell Migration to Defined Lymphoid Organs and Specific Anatomic Compartments of the Spleen. *Cell*. 87:1037–1047. doi:10.1016/S0092-8674(00)81798-5.

Fu, Y.X., G. Huang, Y. Wang, and D.D. Chaplin. 2000. Lymphotoxin-alpha-dependent spleen microenvironment supports the generation of memory B cells and is required for their subsequent antigen-induced activation. *J. Immunol. Baltim. Md 1950*. 164:2508–2514. doi:10.4049/jimmunol.164.5.2508.

Fu, Y.X., H. Molina, M. Matsumoto, G. Huang, J. Min, and D.D. Chaplin. 1997. Lymphotoxin-alpha (LTalpha) supports development of splenic follicular structure that is required for IgG responses. *J. Exp. Med.* 185:2111–2120. doi:10.1084/jem.185.12.2111.

Fukuda, T., T. Yoshida, S. Okada, M. Hatano, T. Miki, K. Ishibashi, S. Okabe, H. Koseki, S. Hirosawa, M. Taniguchi, N. Miyasaka, and T. Tokuhisa. 1997. Disruption of the Bcl6 Gene Results in an Impaired Germinal Center Formation. *J. Exp. Med.* 186:439–448. doi:10.1084/jem.186.3.439.

Galli, S.J., and M. Tsai. 2012. IgE and mast cells in allergic disease. *Nat. Med.* 18:693–704. doi:10.1038/nm.2755.

Garcia-Beltran, W.F., E.C. Lam, K. St. Denis, A.D. Nitido, Z.H. Garcia, B.M. Hauser, J. Feldman, M.N. Pavlovic, D.J. Gregory, M.C. Poznansky, A. Sigal, A.G. Schmidt, A.J. Iafrate, V. Naranbhai, and A.B. Balazs. 2021. Multiple SARS-CoV-2 variants escape neutralization by vaccine-induced humoral immunity. *Cell*. 184:2372-2383.e9. doi:10.1016/j.cell.2021.03.013.

Gitlin, A.D., Z. Shulman, and M.C. Nussenzweig. 2014. Clonal selection in the germinal centre by regulated proliferation and hypermutation. *Nature*. 509:637–640. doi:10.1038/nature13300.

Glick, B., T.S. Chang, and R.G. Jaap. 1956. The Bursa of Fabricius and Antibody Production. *Poult. Sci.* 35:224–225. doi:10.3382/ps.0350224.

Gonzalez, S.F., V. Lukacs-Kornek, M.P. Kuligowski, L.A. Pitcher, S.E. Degn, Y.-A. Kim, M.J. Cloninger, L. Martinez-Pomares, S. Gordon, S.J. Turley, and M.C. Carroll. 2010. Capture of influenza by medullary dendritic cells via SIGN-R1 is essential for humoral immunity in draining lymph nodes. *Nat. Immunol.* 11:427–434. doi:10.1038/ni.1856.

Good-Jacobson, K.L., C.G. Szumilas, L. Chen, A.H. Sharpe, M.M. Tomayko, and M.J. Shlomchik. 2010. PD-1 regulates germinal center B cell survival and the formation and affinity of long-lived plasma cells. *Nat. Immunol.* 11:535–542. doi:10.1038/ni.1877.

Gray, A., and F. Sharara. 2022. Global and regional sepsis and infectious syndrome mortality in 2019: a systematic analysis. *Lancet Glob. Health*. 10:S2. doi:10.1016/S2214-109X(22)00131-0.

Gretz, J.E., C.C. Norbury, A.O. Anderson, A.E.I. Proudfoot, and S. Shaw. 2000. Lymph-Borne Chemokines and Other Low Molecular Weight Molecules Reach High Endothelial Venules via Specialized Conduits While a Functional Barrier Limits Access to the Lymphocyte Microenvironments in Lymph Node Cortex. *J. Exp. Med.* 192:1425–1440. doi:10.1084/jem.192.10.1425.

Gutzeit, C., K. Chen, and A. Cerutti. 2018. The enigmatic function of IgD: some answers at last. *Eur. J. Immunol.* 48:1101–1113. doi:10.1002/eji.201646547.

Hägglöf, T., M. Cipolla, M. Loewe, S.T. Chen, E.E. Kara, L. Mesin, H. Hartweger, M.A. ElTanbouly, A. Cho, A. Gazumyan, V. Ramos, L. Stamatatos, T.Y. Oliveira, M.C. Nussenzweig, and C. Viant. 2023. Continuous germinal center invasion contributes to the diversity of the immune response. *Cell*. 186:147-161.e15. doi:10.1016/j.cell.2022.11.032.

Haley, P.J. 2003. Species differences in the structure and function of the immune system. *Toxicology*. 188:49–71. doi:10.1016/S0300-483X(03)00043-X.

Hickman, D.L., J. Johnson, T.H. Vemulapalli, J.R. Crisler, and R. Shepherd. 2017. Commonly Used Animal Models. *Princ. Anim. Res. Grad. Undergrad. Stud.* 117–175. doi:10.1016/B978-0-12-802151-4.00007-4.

Hillion, S., M.I. Arleevskaya, P. Blanco, A. Bordron, W.H. Brooks, J.Y. Cesbron, S. Kaveri, E. Vivier, and Y. Renaudineau. 2020. The Innate Part of the Adaptive Immune System. *Clin. Rev. Allergy Immunol.* 58:151–154. doi:10.1007/s12016-019-08740-1.

Holt, P.G., and C.A. Jones. 2000. The development of the immune system during pregnancy and early life. *Allergy*. 55:688–697. doi:10.1034/j.1398-9995.2000.00118.x.

Islam, S., A. Zeisel, S. Joost, G. La Manno, P. Zajac, M. Kasper, P. Lönnerberg, and S. Linnarsson. 2014. Quantitative single-cell RNA-seq with unique molecular identifiers. *Nat. Methods*. 11:163–166. doi:10.1038/nmeth.2772.

Jacob, J., G. Kelsoe, K. Rajewsky, and U. Weiss. 1991. Intraclonal generation of antibody mutants in germinal centres. *Nature*. 354:389–392. doi:10.1038/354389a0.

Johnson, L.A., S. Clasper, A.P. Holt, P.F. Lalor, D. Baban, and D.G. Jackson. 2006. An inflammation-induced mechanism for leukocyte transmigration across lymphatic vessel endothelium. *J. Exp. Med.* 203:2763–2777. doi:10.1084/jem.20051759.

Kaji, T., A. Ishige, M. Hikida, J. Taka, A. Hijikata, M. Kubo, T. Nagashima, Y. Takahashi, T. Kurosaki, M. Okada, O. Ohara, K. Rajewsky, and T. Takemori. 2012. Distinct cellular pathways select germline-encoded and somatically mutated antibodies into immunological memory. *J. Exp. Med.* 209:2079–2097. doi:10.1084/jem.20120127.

Kashem, S.W., M. Haniffa, and D.H. Kaplan. 2017. Antigen-Presenting Cells in the Skin. *Annu. Rev. Immunol.* 35:469–499. doi:10.1146/annurev-immunol-051116-052215.

Katzav, S. 2015. Vav1: A Dr. Jekyll and Mr. Hyde protein - good for the hematopoietic system, bad for cancer. *Oncotarget*. 6:28731–28742. doi:10.18632/oncotarget.5086.

Katzav, S., D. Martin-Zanca, and M. Barbacid. 1989. vav, a novel human oncogene derived from a locus ubiquitously expressed in hematopoietic cells. *EMBO J.* 8:2283–2290. doi:10.1002/j.1460-2075.1989.tb08354.x.

Kaur, B.P., and E. Secord. 2019. Innate Immunity. *Pediatr. Clin. North Am.* 66:905–911. doi:10.1016/j.pcl.2019.06.011.

Keyt, B.A., R. Baliga, A.M. Sinclair, S.F. Carroll, and M.S. Peterson. 2020. Structure, Function, and Therapeutic Use of IgM Antibodies. *Antibodies*. 9:53. doi:10.3390/antib9040053.

Klein, U., K. Rajewsky, and R. Küppers. 1998. Human immunoglobulin (Ig)M+IgD+ peripheral blood B cells expressing the CD27 cell surface antigen carry somatically mutated variable region genes: CD27 as a general marker for somatically mutated (memory) B cells. *J. Exp. Med.* 188:1679–1689. doi:10.1084/jem.188.9.1679.

Kumar, B.V., T.J. Connors, and D.L. Farber. 2018. Human T Cell Development, Localization, and Function throughout Life. *Immunity*. 48:202–213. doi:10.1016/j.immuni.2018.01.007.

Kumar, N., C.P. Arthur, C. Ciferri, and M.L. Matsumoto. 2020. Structure of the secretory immunoglobulin A core. *Science*. 367:1008–1014. doi:10.1126/science.aaz5807.

Kurosaki, T., K. Kometani, and W. Ise. 2015. Memory B cells. *Nat. Rev. Immunol.* 15:149–159. doi:10.1038/nri3802.

Laidlaw, B.J., T.H. Schmidt, J.A. Green, C.D.C. Allen, T. Okada, and J.G. Cyster. 2017. The Eph-related tyrosine kinase ligand Ephrin-B1 marks germinal center and memory precursor B cells. *J. Exp. Med.* 214:639–649. doi:10.1084/jem.20161461.

Liu, Y., J. Suckale, J. Masjkur, M.G. Magro, A. Steffen, K. Anastassiadis, and M. Solimena. 2010. Tamoxifen-independent recombination in the RIP-CreER mouse. *PloS One*. 5:e13533. doi:10.1371/journal.pone.0013533.

Lucas, M., U. Karrer, A. Lucas, and P. Klenerman. 2001. Viral escape mechanisms – escapology taught by viruses. *Int. J. Exp. Pathol.* 82:269–286. doi:10.1046/j.1365-2613.2001.00204.x.

Ma, H., and R. O'Kennedy. 2015. The Structure of Natural and Recombinant Antibodies. *Methods Mol. Biol. Clifton NJ*. 1348:7–11. doi:10.1007/978-1-4939-2999-3_2.

MacLennan, I.C.M., K.-M. Toellner, A.F. Cunningham, K. Serre, D.M.-Y. Sze, E. Zúñiga, M.C. Cook, and C.G. Vinuesa. 2003. Extrafollicular antibody responses: MacLennan et al · Extrafollicular antibody responses. *Immunol. Rev.* 194:8–18. doi:10.1034/j.1600-065X.2003.00058.x.

Madisen, L., T.A. Zwingman, S.M. Sunkin, S.W. Oh, H.A. Zariwala, H. Gu, L.L. Ng, R.D. Palmiter, M.J. Hawrylycz, A.R. Jones, E.S. Lein, and H. Zeng. 2010. A robust and high-throughput Cre reporting and characterization system for the whole mouse brain. *Nat. Neurosci.* 13:133–140. doi:10.1038/nn.2467.

Mathenge, V., C. Onuekwe, S. Nass, C. Akim, E. Msunyaro, E. Mfinanga, W.P. Mambo, S.G. Mwabulambo, S. Manozas, D. Kayera, F. Tinuga, S. Tegegne, W. Mwengee, P. Atuhebwe, and Y. Zabulon. 2023. Strategies to improve COVID-19 vaccination coverage in Manyara region, Tanzania, July to September 2022: best practices and lessons learned. *Pan Afr. Med. J.* 45:3. doi:10.11604/pamj.supp.2023.45.1.39608.

Matsumoto, M., S.F. Lo, C.J. Carruthers, J. Min, S. Mariathasan, G. Huang, D.R. Plas, S.M. Martin, R.S. Geha, M.H. Nahm, and D.D. Chaplin. 1996. Affinity maturation without germinal centres in lymphotoxin-alpha-deficient mice. *Nature*. 382:462–466. doi:10.1038/382462a0.

Mayer, C.T., A. Gazumyan, E.E. Kara, A.D. Gitlin, J. Golijanin, C. Viant, J. Pai, T.Y. Oliveira, Q. Wang, A. Escolano, M. Medina-Ramirez, R.W. Sanders, and M.C. Nussenzweig. 2017. The microanatomic segregation of selection by apoptosis in the germinal center. *Science*. 358:eaao2602. doi:10.1126/science.aao2602.

McGuire, A.T., M.D. Gray, P. Dosenovic, A.D. Gitlin, N.T. Freund, J. Petersen, C. Correnti, W. Johnsen, R. Kegel, A.B. Stuart, J. Glenn, M.S. Seaman, W.R. Schief, R.K. Strong, M.C. Nussenzweig, and L. Stamatatos. 2016. Specifically modified Env immunogens activate B-cell precursors of broadly neutralizing HIV-1 antibodies in transgenic mice. *Nat. Commun.* 7:10618. doi:10.1038/ncomms10618.

McHeyzer-Williams, L.J., M. Cool, and M.G. McHeyzer-Williams. 2000. Antigen-specific B cell memory: expression and replenishment of a novel b220(-) memory b cell compartment. *J. Exp. Med.* 191:1149–1166. doi:10.1084/jem.191.7.1149.

Mestas, J., and C.C.W. Hughes. 2004. Of Mice and Not Men: Differences between Mouse and Human Immunology. *J. Immunol.* 172:2731–2738. doi:10.4049/jimmunol.172.5.2731.

Mondal, A., D. Sawant, and A.L. Dent. 2010. Transcriptional repressor BCL6 controls Th17 responses by controlling gene expression in both T cells and macrophages. *J. Immunol. Baltim. Md 1950*. 184:4123–4132. doi:10.4049/jimmunol.0901242.

Morens, D.M., and A.S. Fauci. 2020. Emerging Pandemic Diseases: How We Got to COVID-19. *Cell*. 182:1077–1092. doi:10.1016/j.cell.2020.08.021.

Msemburi, W., A. Karlinsky, V. Knutson, S. Aleshin-Guendel, S. Chatterji, and J. Wakefield. 2023. The WHO estimates of excess mortality associated with the COVID-19 pandemic. *Nature*. 613:130–137. doi:10.1038/s41586-022-05522-2.

Muramatsu, M., K. Kinoshita, S. Fagarasan, S. Yamada, Y. Shinkai, and T. Honjo. 2000. Class Switch Recombination and Hypermutation Require Activation-Induced Cytidine Deaminase (AID), a Potential RNA Editing Enzyme. *Cell*. 102:553–563. doi:10.1016/S0092-8674(00)00078-7.

Murphy, K., and C. Weaver. 2018. Janeway Immunologie. 9th edition. Springer Spektrum, Heidelberg. 1207 pp.

Nieuwenhuis, P., and D. Opstelten. 1984. Functional anatomy of germinal centers. *Am. J. Anat.* 170:421–435. doi:10.1002/aja.1001700315.

Nutt, S.L., P.D. Hodgkin, D.M. Tarlinton, and L.M. Corcoran. 2015. The generation of antibody-secreting plasma cells. *Nat. Rev. Immunol.* 15:160–171. doi:10.1038/nri3795.

Ogilvy, S., A.G. Elefanty, J. Visvader, M.L. Bath, A.W. Harris, and J.M. Adams. 1998. Transcriptional Regulation of vav, a Gene Expressed Throughout the Hematopoietic Compartment. *Blood*. 91:419–430. doi:10.1182/blood.V91.2.419.

Ohtsuka, H., A. Sakamoto, J. Pan, S. Inage, S. Horigome, H. Ichii, M. Arima, M. Hatano, S. Okada, and T. Tokuhisa. 2011. Bcl6 Is Required for the Development of Mouse CD4+ and CD8α+ Dendritic Cells. *J. Immunol.* 186:255–263. doi:10.4049/jimmunol.0903714.

Okada, T., M.J. Miller, I. Parker, M.F. Krummel, M. Neighbors, S.B. Hartley, A. O'Garra, M.D. Cahalan, and J.G. Cyster. 2005. Antigen-Engaged B Cells Undergo Chemotaxis toward the T Zone and Form Motile Conjugates with Helper T Cells. *PLoS Biol.* 3:e150. doi:10.1371/journal.pbio.0030150.

Pal, G.K. 2006. Textbook Of Practical Physiology. 2nd edition. Orient Blackswan, Hyderabad. 456 pp.

Pape, K.A., D.M. Catron, A.A. Itano, and M.K. Jenkins. 2007. The Humoral Immune Response Is Initiated in Lymph Nodes by B Cells that Acquire Soluble Antigen Directly in the Follicles. *Immunity*. 26:491–502. doi:10.1016/j.immuni.2007.02.011.

Pape, K.A., J.J. Taylor, R.W. Maul, P.J. Gearhart, and M.K. Jenkins. 2011. Different B cell populations mediate early and late memory during an endogenous immune response. *Science*. 331:1203–1207. doi:10.1126/science.1201730.

Parker, D.C. 1993. T Cell-Dependent B Cell Activation. *Annu. Rev. Immunol.* 11:331–360. doi:10.1146/annurev.iy.11.040193.001555.

Paus, D., T.G. Phan, T.D. Chan, S. Gardam, A. Basten, and R. Brink. 2006. Antigen recognition strength regulates the choice between extrafollicular plasma cell and germinal center B cell differentiation. *J. Exp. Med.* 203:1081–1091. doi:10.1084/jem.20060087.

Plotkin, S.A. 2010. Correlates of Protection Induced by Vaccination. *Clin. Vaccine Immunol.* 17:1055–1065. doi:10.1128/CVI.00131-10.

Polack, F.P., J. Absalon, J.L. Perez, C. Zerbini, S. Roychoudhury, W.V. Kalina, L.L. Hammitt, S. Ünal, P.R. Dormitzer, and W.C. Gruber. 2020. Safety and Efficacy of the BNT162b2 mRNA Covid-19 Vaccine. *N Engl J Med*. 13. doi:10.1056/NEJMoa2034577.

Popescu, D.-M., R.A. Botting, E. Stephenson, K. Green, S. Webb, L. Jardine, E.F. Calderbank, K. Polanski, I. Goh, M. Efremova, M. Acres, D. Maunder, P. Vegh, Y. Gitton, J.-E. Park, R. Vento-Tormo, Z. Miao, D. Dixon, R. Rowell, D. McDonald, J. Fletcher, E. Poyner, G. Reynolds, M. Mather, C. Moldovan, L. Mamanova, F. Greig, M. Young, K.B. Meyer, S. Lisgo, J. Bacardit, A. Fuller, B. Millar, B. Innes, S. Lindsay, M.J.T. Stubbington, M.S. Kowalczyk, B. Li, O. Ashenbrg, M. Tabaka, D. Dionne, T.L. Tickle, M. Slyper, O. Rozenblatt-Rosen, A. Filby, P. Carey, A.-C. Villani, A. Roy, A. Regev, A. Chedotal, I. Roberts, B. Göttgens, S. Behjati, E. Laurenti, S.A. Teichmann, and M. Haniffa. 2019. Decoding human fetal liver haematopoiesis. *Nature*. 574:365–371. doi:10.1038/s41586-019-1652-y.

Porto, J.M.D., A.M. Haberman, M.J. Shlomchik, and G. Kelsoe. 1998. Antigen Drives Very Low Affinity B Cells to Become Plasmacytes and Enter Germinal Centers. *J. Immunol.* 161:5373–5381.

Purtha, W.E., T.F. Tedder, S. Johnson, D. Bhattacharya, and M.S. Diamond. 2011. Memory B cells, but not long-lived plasma cells, possess antigen specificities for viral escape mutants. *J. Exp. Med.* 208:2599–2606. doi:10.1084/jem.20110740.

Qatarneh, S.M., I.-C. Kiricuta, A. Brahme, U. Tiede, and B.K. Lind. 2006. Three-dimensional atlas of lymph node topography based on the visible human data set. *Anat. Rec. B. New Anat.* 289B:98–111. doi:10.1002/ar.b.20102.

Qi, H., J.G. Egen, A.Y.C. Huang, and R.N. Germain. 2006. Extrafollicular Activation of Lymph Node B Cells by Antigen-Bearing Dendritic Cells. *Science*. 312:1672–1676. doi:10.1126/science.1125703.

Rajewsky, K. 1996. Clonal selection and learning in the antibody system. *Nature*. 381:751–758. doi:10.1038/381751a0.

Randolph, G.J., V. Angeli, and M.A. Swartz. 2005. Dendritic-cell trafficking to lymph nodes through lymphatic vessels. *Nat. Rev. Immunol.* 5:617–628. doi:10.1038/nri1670.

Ridderstad, A., and D.M. Tarlinton. 1998. Kinetics of establishing the memory B cell population as revealed by CD38 expression. *J. Immunol. Baltim. Md 1950*. 160:4688–4695.

Roco, J.A., L. Mesin, S.C. Binder, C. Nefzger, P. Gonzalez-Figueroa, P.F. Canete, J. Ellyard, Q. Shen, P.A. Robert, J. Cappello, H. Vohra, Y. Zhang, C.R. Nowosad, A. Schiepers, L.M. Corcoran, K.-M. Toellner, J.M. Polo, M. Meyer-Hermann, G.D. Victora, and C.G. Vinuesa. 2019. Class-Switch Recombination Occurs Infrequently in Germinal Centers. *Immunity*. 51:337-350.e7. doi:10.1016/j.immuni.2019.07.001.

Roeder, P., J. Mariner, and R. Kock. 2013. Rinderpest: the veterinary perspective on eradication. *Philos. Trans. R. Soc. B Biol. Sci.* 368:20120139. doi:10.1098/rstb.2012.0139.

Roitt, I.M., G. Torrigiani, M.F. Greaves, J. Brostoff, and J.H.L. Playfair. 1969. The Cellular Basis of Immunological Responses. *The Lancet*. 294:367–371. doi:10.1016/S0140-6736(69)92712-3.

Ruddle, N.H., and E.M. Akirav. 2009. Secondary Lymphoid Organs: Responding to Genetic and Environmental Cues in Ontogeny and the Immune Response. *J. Immunol. Baltim. Md 1950*. 183:2205–2212. doi:10.4049/jimmunol.0804324.

Santambrogio, L. 2013. Immunology of the Lymphatic System. 1st edition. Springer, New York. 177 pp.

Scallan, J.P., S.D. Zawieja, J.A. Castorena-Gonzalez, and M.J. Davis. 2016. Lymphatic pumping: mechanics, mechanisms and malfunction: Lymphatic pumping mechanisms. *J. Physiol.* 594:5749–5768. doi:10.1113/JP272088.

Scheid, J.F., H. Mouquet, N. Feldhahn, M.S. Seaman, K. Velinzon, J. Pietzsch, R.G. Ott, R.M. Anthony, H. Zebroski, A. Hurley, A. Phogat, B. Chakrabarti, Y. Li, M. Connors, F. Pereyra, B.D. Walker, H. Wardemann, D. Ho, R.T. Wyatt, J.R. Mascola, J.V. Ravetch, and M.C. Nussenzweig. 2009. Broad diversity of neutralizing antibodies isolated from memory B cells in HIV-infected individuals. *Nature*. 458:636–640. doi:10.1038/nature07930.

Schwickert, T.A., G.D. Victora, D.R. Fooksman, A.O. Kamphorst, M.R. Mugnier, A.D. Gitlin, M.L. Dustin, and M.C. Nussenzweig. 2011. A dynamic T cell–limited checkpoint regulates affinity-dependent B cell entry into the germinal center. *J. Exp. Med.* 208:1243–1252. doi:10.1084/jem.20102477.

Shaffer, A.L., X. Yu, Y. He, J. Boldrick, E.P. Chan, and L.M. Staudt. 2000. BCL-6 represses genes that function in lymphocyte differentiation, inflammation, and cell cycle control. *Immunity*. 13:199–212. doi:10.1016/s1074-7613(00)00020-0.

Shinnakasu, R., T. Inoue, K. Kometani, S. Moriyama, Y. Adachi, M. Nakayama, Y. Takahashi, H. Fukuyama, T. Okada, and T. Kurosaki. 2016. Regulated selection of germinal-center cells into the memory B cell compartment. *Nat. Immunol.* 17:861–869. doi:10.1038/ni.3460.

Suan, D., N.J. Kräutler, J.L.V. Maag, D. Butt, K. Bourne, J.R. Hermes, D.T. Avery, C. Young, A. Statham, M. Elliott, M.E. Dinger, A. Basten, S.G. Tangye, and R. Brink. 2017. CCR6 Defines Memory B Cell Precursors in Mouse and Human

Germinal Centers, Revealing Light-Zone Location and Predominant Low Antigen Affinity. *Immunity*. 47:1142-1153.e4. doi:10.1016/j.immuni.2017.11.022.

Suzuki, K., I. Grigorova, T.G. Phan, L.M. Kelly, and J.G. Cyster. 2009. Visualizing B cell capture of cognate antigen from follicular dendritic cells. *J. Exp. Med.* 206:1485–1493. doi:10.1084/jem.20090209.

Swartzendruber, D.C., and C.C. Congdon. 1963. Electron Microscope Observations on Tingible Body Macrophages in Mouse Spleen. *J. Cell Biol.* 19:641–646. doi:10.1083/jcb.19.3.641.

Tangye, S.G., and K.L. Good. 2007. Human IgM $^{+}$ CD27 $^{+}$ B Cells: Memory B Cells or "Memory" B Cells? *J. Immunol.* 179:13–19. doi:10.4049/jimmunol.179.1.13.

Taylor, A.E., W.H. Gibson, H.J. Granger, and A.C. Guyton. 1973. The interaction between intracapillary and tissue forces in the overall regulation of interstitial fluid volume. *Lymphology*. 6:192–208.

Taylor, J.J., K.A. Pape, and M.K. Jenkins. 2012. A germinal center–independent pathway generates unswitched memory B cells early in the primary response. *J. Exp. Med.* 209:597–606. doi:10.1084/jem.20111696.

Toyama, H., S. Okada, M. Hatano, Y. Takahashi, N. Takeda, H. Ichii, T. Takemori, Y. Kuroda, and T. Tokuhisa. 2002. Memory B Cells without Somatic Hypermutation Are Generated from Bcl6-Deficient B Cells. *Immunity*. 17:329–339. doi:10.1016/S1074-7613(02)00387-4.

Trombetta, J.J., D. Gennert, D. Lu, R. Satija, A.K. Shalek, and A. Regev. 2014. Preparation of Single-Cell RNA-Seq Libraries for Next Generation Sequencing. *Curr. Protoc. Mol. Biol.* 107. doi:10.1002/0471142727.mb0422s107.

Valenzuela, N.M., and S. Schaub. 2018. The Biology of IgG Subclasses and Their Clinical Relevance to Transplantation. *Transplantation*. 102:S7–S13. doi:10.1097/TP.0000000000001816.

Van den Broeck, W., A. Derore, and P. Simoens. 2006. Anatomy and nomenclature of murine lymph nodes: Descriptive study and nomenclatory standardization in BALB/cAnNCrl mice. *J. Immunol. Methods*. 312:12–19. doi:10.1016/j.jim.2006.01.022.

Viant, C., T. Wirthmiller, M.A. ElTanbouly, S.T. Chen, E.E. Kara, M. Cipolla, V. Ramos, T.Y. Oliveira, L. Stamatatos, and M.C. Nussenzweig. 2021. Germinal center-dependent and -independent memory B cells produced throughout the immune response. *J. Exp. Med.* 218:e20202489. doi:10.1084/jem.20202489.

Victora, G.D., and M.C. Nussenzweig. 2012. Germinal Centers. *Annu. Rev. Immunol.* 30:429–457. doi:10.1146/annurev-immunol-020711-075032.

Victora, G.D., T.A. Schwickert, D.R. Fooksman, A.O. Kamphorst, M. Meyer-Hermann, M.L. Dustin, and M.C. Nussenzweig. 2010. Germinal Center Dynamics Revealed

by Multiphoton Microscopy with a Photoactivatable Fluorescent Reporter. *Cell*. 143:592–605. doi:10.1016/j.cell.2010.10.032.

Vitetta, E.S., R. Fernandez-Botran, C.D. Myers, and V.M. Sanders. 1989. Cellular interactions in the humoral immune response. *Adv. Immunol.* 45:1–105. doi:10.1016/s0065-2776(08)60692-6.

Vos, Q., A. Lees, Z.Q. Wu, C.M. Snapper, and J.J. Mond. 2000. B-cell activation by T-cell-independent type 2 antigens as an integral part of the humoral immune response to pathogenic microorganisms. *Immunol. Rev.* 176:154–170. doi:10.1034/j.1600-065x.2000.00607.x.

Weisel, F., and M. Shlomchik. 2017. Memory B Cells of Mice and Humans. *Annu. Rev. Immunol.* 35:255–284. doi:10.1146/annurev-immunol-041015-055531.

Weisel, F.J., G.V. Zuccarino-Catania, M. Chikina, and M.J. Shlomchik. 2016. A Temporal Switch in the Germinal Center Determines Differential Output of Memory B and Plasma Cells. *Immunity*. 44:116–130. doi:10.1016/j.immuni.2015.12.004.

West, H.C., and C.L. Bennett. 2017. Redefining the Role of Langerhans Cells As Immune Regulators within the Skin. *Front. Immunol.* 8:1941. doi:10.3389/fimmu.2017.01941.

Willard-Mack, C.L. 2006. Normal Structure, Function, and Histology of Lymph Nodes. *Toxicol. Pathol.* 34:409–424. doi:10.1080/01926230600867727.

Woolhouse, M.E.J., and S. Gowtage-Sequeria. 2005. Host Range and Emerging and Reemerging Pathogens. *Emerg. Infect. Dis.* 11:1842–1847. doi:10.3201/eid1112.050997.

Ye, B.H., G. Cattoretti, Q. Shen, J. Zhang, N. Hawe, R.D. Waard, C. Leung, M. Nouri-Shirazi, A. Orazi, R.S.K. Chaganti, P. Rothman, A.M. Stall, P.-P. Pandolfi, and R. Dalla-Favera. 1997. The BCL-6 proto-oncogene controls germinal-centre formation and Th2-type inflammation. *Nat. Genet.* 16:161–170. doi:10.1038/ng0697-161.

Acknowledgments

I would like to thank the following people who have helped me to complete this thesis: Ludger Klein who accepted me as his doctoral student and supported me throughout the years of the process. Michel Nussenzweig who hosted me as a research student in his lab and took good care of me so I could fully focus on my experiments. Michael Meyer who introduced me to research during my preclinical studies and mentored me throughout medical school and my doctorate with an open ear to my countless questions. Charlotte Viant who supervised and taught me patiently during my research stay. My colleagues at Rockefeller University for all their help. Nikolas, Nina, Marta, Tobias, Florian, Tarek and Anne who provided me with excellent advice and friendship. My parents, siblings and grandparents for making all of this possible.

Affidavit

LMU LUDWIG-MAXIMILIANS-UNIVERSITÄT MÜNCHEN | Promotionsbüro Medizinische Fakultät | MMRS

Eidesstattliche Versicherung

Wirthmiller, Tobias

Name, Vorname

Ich erkläre hiermit an Eides statt, dass ich die vorliegende Dissertation mit dem Titel:

The Origin of Memory B Cells

selbständig verfasst, mich außer der angegebenen keiner weiteren Hilfsmittel bedient und alle Erkenntnisse, die aus dem Schrifttum ganz oder annähernd übernommen sind, als solche kenntlich gemacht und nach ihrer Herkunft unter Bezeichnung der Fundstelle einzeln nachgewiesen habe.

Ich erkläre des Weiteren, dass die hier vorgelegte Dissertation nicht in gleicher oder in ähnlicher Form bei einer anderen Stelle zur Erlangung eines akademischen Grades eingereicht wurde.

Hallein, 14.09.2024
Ort, Datum

Tobias Wirthmiller
Unterschrift Doktorandin bzw. Doktorand

List of Publications

1. Viant C, **Wirthmiller T**, ElTanbouly MA, et al. Germinal center-dependent and -independent memory B cells produced throughout the immune response. *J Exp Med*. 2021;218(8):e20202489. doi:10.1084/jem.20202489
2. **Wirthmiller TB**, Neu BU, Schmitz FM, Wohlfarth B. NEPTUNE. On the seven seas of resilience. *Med Educ Online*. 2023;28(1):2246782. doi:10.1080/10872981.2023.2246782